The Plant Cell, Vol. 26: 2038–2054, May 2014, www.plantcell.org © 2014 American Society of Plant Biologists. All rights reserved.

A Zinc Finger Protein Regulates Flowering Time and Abiotic Stress Tolerance in Chrysanthemum by Modulating Gibberellin Biosynthesis[C][W][OPEN]

Yingjie Yang,[a] Chao Ma,[a] Yanjie Xu,[a] Qian Wei,[a] Muhammad Imtiaz,[a] Haibo Lan,[a] Shan Gao,[b,c] Lina Cheng,[a] Meiyan Wang,[a] Zhangjun Fei,[b,c] Bo Hong,[a] and Junping Gao[a,1]

[a] Department of Ornamental Horticulture, China Agricultural University, 100193 Beijing, China
[b] Boyce Thompson Institute for Plant Research, Cornell University, Ithaca, New York 14853
[c] U.S. Department of Agriculture Robert W. Holley Center for Agriculture and Health, Ithaca, New York 14853

Flowering time and an ability to tolerate abiotic stresses are important for plant growth and development. We characterized *BBX24*, a zinc finger transcription factor gene, from *Chrysanthemum morifolium* and found it to be associated with both flowering time and stress tolerance. Transgenic lines with suppressed expression of Cm-*BBX24* (Cm-*BBX24*-RNAi) flowered earlier than wild-type plants and showed decreased tolerance to freezing and drought stresses. Global expression analysis revealed that genes associated with both photoperiod and gibberellin (GA) biosynthesis pathways were upregulated in Cm-*BBX24*-RNAi lines, relative to the wild type. By contrast, genes that were upregulated in overexpressing lines (Cm-*BBX24*-OX), but downregulated in Cm-*BBX24*-RNAi lines (both relative to the wild type), included genes related to compatible solutes and carbohydrate metabolism, both of which are associated with abiotic stress. Cm-*BBX24* expression was also influenced by daylength and $GA_{4/7}$ application. Under long days, changes in endogenous GA_1, GA_4, GA_{19}, and GA_{20} levels occurred in young leaves of transgenic lines, relative to the wild type. Regulation of flowering involves the *FLOWERING TIME* gene, which integrates photoperiod and GA biosynthesis pathways. We postulate that Cm-*BBX24* plays a dual role, modulating both flowering time and abiotic stress tolerance in chrysanthemum, at least in part by influencing GA biosynthesis.

INTRODUCTION

Flowering at the appropriate time of year is essential for successful reproduction and also has commercial significance for crops and ornamental plants. Flowering time is determined by external environmental cues and endogenous developmental signals (Lang 1965; Fornara et al., 2010). Plants have been shown to utilize various and often interconnecting flowering mechanisms, including photoperiod, vernalization, gibberellin (GA) biosynthesis, and aging pathways (Song et al., 2013). Outputs from these pathways are integrated by a set of common downstream flowering-time integrators, such as *FLOWERING LOCUS T* (*FT*) and *SUPPRESSOR OF OVEREXPRESSION OF CO1* (*SOC1*), whose expression leads to the induction of floral meristem identity genes, including *LEAFY* (*LFY*) and *APETALA1* and, consequently, flowering (Song et al., 2013).

Plants can be classified as long-day (LD), short-day (SD), or day-neutral based on daylength requirements for flowering (Lang, 1965; Srikanth and Schmid, 2011). A core component of the photoperiod pathway is CONSTANS (CO), a gene that upregulates the immediate downstream genes *FT* and *SOC1* (Samach et al., 2000). CO is classified as a B-box protein and was the first such protein identified from *Arabidopsis thaliana* (Putterill et al., 1995). The B-box is a zinc finger binding domain consisting of conserved Cys and His residues, and proteins with one or two B-boxes in the N-terminal region are all classed as transcription factors and termed BBX, according to the nomenclature proposed for *Arabidopsis* (Khanna et al., 2009). In *Arabidopsis*, the BBX family has 32 members and is divided into five structural groups, based on the number and sequence features of the B-box domain and whether the protein also contains a CCT domain (Khanna et al., 2009). Structure group I has six members (CO, also known as BBX1, and BBX2 to 6), each of which contains two B-box domains and a CCT domain. Structure group II has seven members (BBX7 to 13), which are structurally similar to group I but have differences in their second B-box domain. Structure group III has four members (BBX14 to 17) characterized by having only one B-box domain and a CCT domain. BBX2 to 17 are all CO-LIKE (COL) proteins. Structure group IV has eight members (BBX18 to 25), which contain two B-box domains but have no CCT domain. Lastly, structure group V has seven members (BBX26 to 32), each of which has just a single B-box domain (Khanna et al., 2009).

It has been demonstrated that some members of structure groups I and III act to regulate flowering time. Of these, CO (BBX1) is the best-characterized BBX member, acting as a transcription factor in the photoperiodic pathway's regulation of flowering time (Putterill et al., 1995). Additionally, *COL* genes are known to be associated with the positive or negative regulation of

[1] Address correspondence to gaojp@cau.edu.cn.
The author responsible for distribution of materials integral to the findings presented in this article in accordance with the policy described in the Instructions for Authors (www.plantcell.org) is: Junping Gao (gaojp@cau.edu.cn).
[C] Some figures in this article are displayed in color online but in black and white in the print edition.
[W] Online version contains Web-only data.
[OPEN] Articles can be viewed online without a subscription.
www.plantcell.org/cgi/doi/10.1105/tpc.114.124867

flowering time. For example, *COL5* (*BBX6*) can induce flowering in *Arabidopsis* (Hassidim et al., 2009), while *COL3* (*BBX4*) expression delays flowering (Cheng and Wang, 2005). In rice (*Oryza sativa*), *Heading date 1*, the ortholog of *Arabidopsis CO*, shortens time to heading (Yano et al., 2000), while Os-*CO3* delays flowering (Kim et al., 2008). *Arabidopsis* plants with a mutation in the *eip6* (*bbx32*) gene, which encodes a member of structure group V, display earlier flowering and increased expression of flowering time and floral organ identity genes, while plants overexpressing *EMF1-Interacting Protein 6* (*BBX32*) show late-flowering phenotypes (Park et al., 2011). However, less is known about BBXs from structure group IV, with regard to their ability to modulate other flowering-related pathways.

Induction of flowering and shortening of time to flowering is also promoted in many plant species by application of GAs, as was initially demonstrated by application of GA_3 to *Arabidopsis* (Langridge, 1957), and it has subsequently been shown that changes in GA biosynthesis and signaling are involved in the regulation of flowering in *Arabidopsis* and *Lolium temulentum* (Srikanth and Schmid, 2011). Gibberellin A_{12}, an early GA in the biosynthesis pathway, is converted to bioactive GA_4 via GA_{15}, GA_{24}, and GA_9 (in the early non-hydroxylation pathway) or to bioactive GA_1 via GA_{53}, GA_{44}, GA_{19}, and GA_{20} (in the early C-13-hydroxylation pathway; Yamaguchi, 2008). Two 2-oxoglutarate–dependent dioxygenases GA 20-oxidase (GA20ox) and GA 3-oxidase (GA3ox) catalyze the formation of these bioactive GAs (Olszewski et al., 2002).

A mechanistic basis for the interaction between the photoperiodic and GA biosynthesis pathways is hinted at by the convergence of both pathways on the promotion of *FT* and *SOC1* transcription in the meristem of *Arabidopsis* (Moon et al., 2003; Porri et al., 2012). In the LD plant *Arabidopsis*, mutations that inhibit the GA biosynthesis pathway or increase the degradation of GAs can delay flowering in SD (Fornara et al. 2010). Conversely, application of florigenic GA structures or overexpression of GA biosynthesis pathway genes leads to early flowering phenotypes in *Arabidopsis* by activating *SOC1* and its target gene *LFY* (Blázquez et al., 1998; Moon et al., 2003). However, to date, little is known about the possible regulation of flowering time by members of the BBX gene family and specifically in association with the GA biosynthesis pathway, especially for SD-requiring plant species.

In addition to flowering time, another crucial factor that can limit plant growth and productivity are environmental stresses, such as those induced by low temperature, drought, and salinity. These abiotic stresses can induce physiological and biochemical changes in plants, changes that are apparent as a broad range of adaptive responses (Hirayama and Shinozaki, 2010). Many of these responses have been associated with transcriptional regulation, and it appears that various transcription factors play a causal role in the tolerance of plants to abiotic stresses. Well-characterized examples include members of the Dehydration-Responsive Element Binding (DREB) protein, NAM ATAF CUC2, MYB, MYC, WRKY, and zinc finger protein transcription factor classes. These transcription factors can variously function as transcriptional activators or repressors and govern downstream gene expression either cooperatively or independently in stress signaling (Hirayama and Shinozaki, 2010).

Several reports have also described the involvements of BBX proteins in abiotic stress tolerance. In *Arabidopsis*, the transcripts of *BBX1-3*, *BBX6-9*, *BBX11*, *BBX13-14*, *BBX16*, *BBX29*, *BBX31*, and structure group IV members *BBX18-19*, *BBX22, BBX24* (*STO*), and *BBX25* (*STH1*/*STH*) are all induced by low temperature (Winter et al., 2007). Similarly, in banana (*Musa nana*), the abundance of Ma-*COL1* transcripts, from structure group I, increases in response to chilling (J. Chen et al., 2012), as does grapevine (*Vitis vinifera*) *ZFPL*, which is an ortholog of *Arabidopsis BBX32* from structure group V, whose overexpression can enhance cold tolerance (Takuhara et al., 2011). Another BBX protein associated with abiotic stress is BBX24, which was initially described as a protein complementing the salt-sensitive phenotype of yeast calcineurin null mutants *cna1*, *cna2*, and *cnb1*, and a yeast calcium channel-deficient mutant, *cch1* (Lippuner et al., 1996). In *Arabidopsis* seedlings, the overexpression of *BBX24* (*STO*) enhances root growth on a high salt medium (Nagaoka and Takano, 2003). However, to date, other than these few examples, there is limited information concerning possible regulatory mechanisms of abiotic stress tolerance being associated with BBX family members.

Chrysanthemum (*Chrysanthemum morifolium*), a commercially important ornamental plant worldwide, is a plant in which SD hastens time to flowering. The annual commercial production of flowering chrysanthemum plants depends mainly on artificial regulation of daylength (Cockshull, 1985). Abiotic stresses, such as low temperature and drought, can be major impediments to the growth, development, and ornamental traits of chrysanthemum and can thus limit productivity. Elucidation of the molecular mechanisms of time to flowering and abiotic stress tolerance is therefore of considerable importance. In this study, we report that Cm-*BBX24*, a zinc finger transcription factor gene from chrysanthemum, plays dual roles in the regulation of flowering time and abiotic stress tolerance: the former by influencing the expression of genes related to the photoperiod pathway and the biosynthesis of endogenous GAs and the latter (abiotic stress tolerance) by being associated with a range of stress response mechanisms.

RESULTS

Isolation of Chrysanthemum *BBX24*

To investigate the function of *BBX* genes in chrysanthemum, we identified a *BBX* homolog with a predicted open reading frame (ORF) of 738 bp that encodes a deduced protein of 245 amino acids. A BLASTP search showed that the deduced polypeptide has similarity to BBX proteins from a range of plant species and contains all of the characteristics of structure group IV members of the BBX family: a highly conserved double B-box domain in the N terminus but no CCT domain in the C terminus (Figure 1A). Phylogenetic analysis of BBX proteins from a range of plant species revealed the predicted protein to cluster with structure group IV BBX homologs from *Arabidopsis* and that this gene is a homolog of At-*BBX24* and At-*BBX25* (Figure 1B), with the greatest similarity to At-*BBX24*. Accordingly, we designated the gene as Cm-*BBX24*, following the nomenclature system suggested by Khanna et al. (2009).

To investigate the potential role of Cm-*BBX24* in regulating time to flowering, we evaluated its expression in different organs,

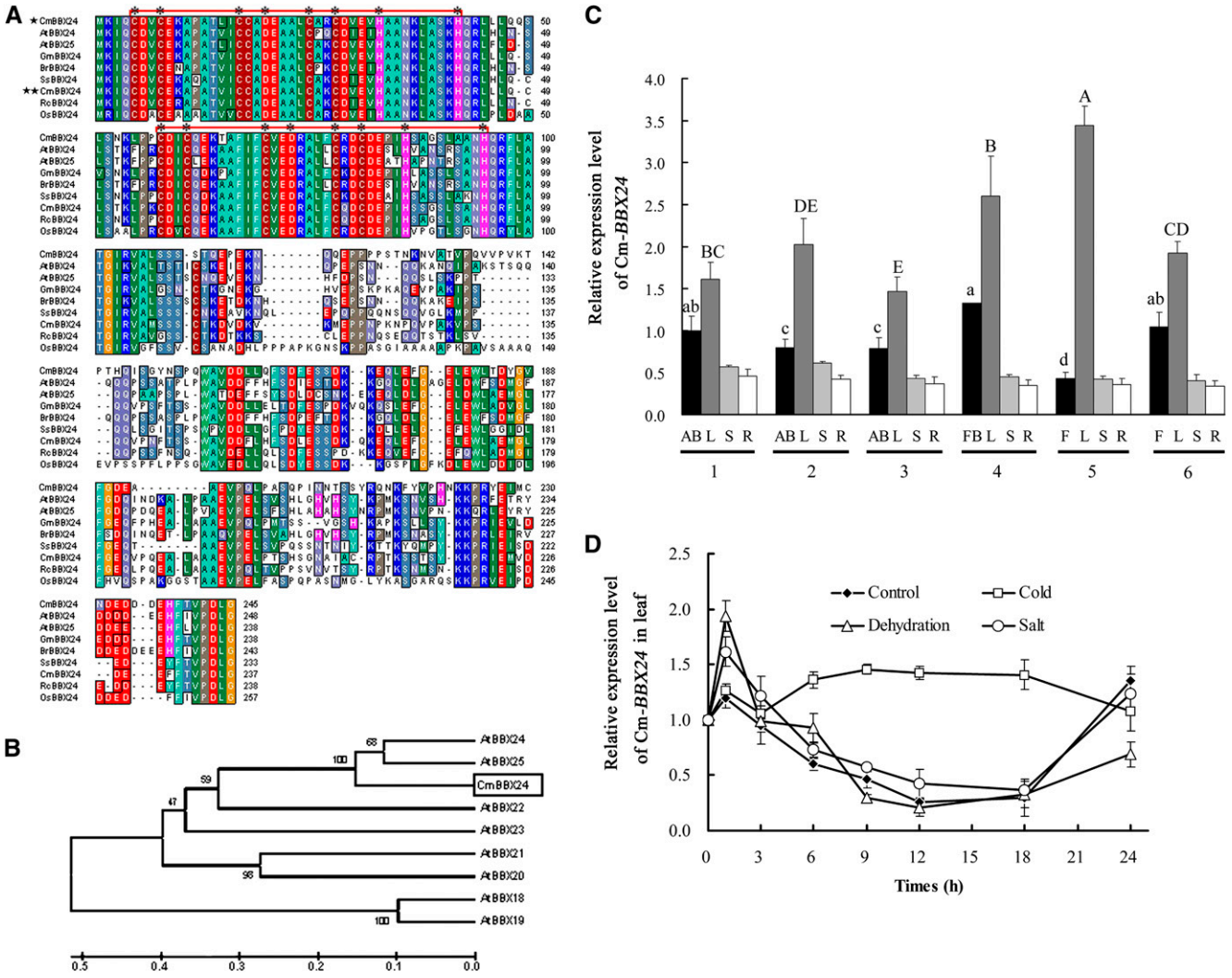

Figure 1. Comparison of Deduced Amino Acid Sequences of Cm-BBX24 with BBXs from Other Plant Species and Expression Patterns of Cm-*BBX24* in Chrysanthemum.

(A) Alignment of deduced amino acid sequences of Cm-BBX24 with other plant BBXs, with conserved amino acids shaded in different colors. The stars before Cm-BBX24 indicate the deduced protein sequence from chrysanthemum and melon (*Cucumis melo*), respectively. Red lines indicate two conserved B-box domains (B1 and B2), and the asterisks indicate the Zn^{2+}-ligating conserved Cys, His, and Asp residues present in the B-box.

(B) Phylogenetic analysis of Cm-BBX24 and eight other structure group IV BBXs from *Arabidopsis*. Bootstrap values indicate the divergence of each branch and the scale indicates branch length.

(C) Expression of Cm-*BBX24* in different tissues at various developmental periods. 1, young plant; 2, mature plant before differentiation; 3, initial period of flower bud differentiation; 4, visible capitulum; 5, initial flowering; 6, flowering; AB, apical buds; L, leaves; S, stems; R, roots; FB, flower buds; F, flowers. *Ubiquitin* was used as the control. Error bars indicate SD ($n = 3$). Significant differences were analyzed by Duncan's multiple range test ($P < 0.05$).

(D) Expression of Cm-*BBX24* under cold, dehydration and salt stress conditions. Error bars indicate SD ($n = 3$).

[See online article for color version of this figure.]

including apical buds, flower buds, leaves, stems, and roots at different vegetative and reproductive growth stages, by quantitative RT-PCR (qRT-PCR). Cm-*BBX24* transcripts were detected in all organs and at all developmental stages tested, and expression in leaves and apical buds, including flower buds, showed significant changes during development, with relatively high transcript abundance in young plants, a decrease in mature plants prior to flower bud differentiation, and a further decrease during the initial period of flower bud differentiation, i.e., prior to the time when the capitulum first becomes visible (Figure 1C). These results suggest that during plant development a temporal decrease of Cm-*BBX24* expression in leaves and apical buds might be associated with the beginning of flower bud differentiation.

To characterize the regulation of Cm-*BBX24* expression, we isolated ~2.7 kb of genomic DNA sequence upstream of the Cm-*BBX24* coding sequence. Analysis of putative *cis*-regulatory

elements using the PLACE database (Supplemental Figure 1A) revealed that the promoter contains predicted flowering-related *cis*-elements, such as CARG, and motifs that are associated with plant hormones (GARE/CARE, GAs; ABRE, abscisic acid), light (T-BOX, GT-1, circadian, and CCA1), and abiotic stress–related (DRE, MYC, and MYB) signaling. The presence of various potential *cis*-elements in the upstream region of Cm-*BBX24* suggested that the gene is regulated by multiple external environmental and internal hormonal cues. In addition, β-glucuronidase activity of the Cm-*BBX24* promoter in *Arabidopsis* was significantly enhanced by treatment with $GA_{4/7}$, cold, and mannitol and was slightly induced by abscisic acid and NaCl treatments (Supplemental Figure 1B).

We then investigated whether the expression of the Cm-*BBX24* in leaves is under the regulation of a circadian clock. The results showed that transcript levels of Cm-*BBX24* oscillated, with a peak occurring at about ZT3 (Zeitgeber time 3 from light), followed by a second peak ~24 h later (ZT27) and a third peak ~48 h later (Supplemental Figure 2A). This indicates that Cm-*BBX24* exhibits a robust free-running circadian rhythm.

The possible involvement of Cm-*BBX24* in abiotic stress responses was assessed by exposing young plants to dehydration, low temperature (4°C), and salt conditions. Under dehydrating conditions, Cm-*BBX24* transcripts showed a rapid and transient induction in leaves (Figure 1D), amounting to an ~1.6-fold increase at the 1-h time point, relative to untreated control plants. Low-temperature treatment also induced expression after 3 h, with further increased expression maintained through 18 h. Salt stress conditions elicited a slight induction of expression in leaves at the 1-h time point. These results indicated that gene transcription was inducible by both low temperature and dehydration.

We further assessed the expression of Cm-*BBX24* in chrysanthemum wild-type plants under different daylengths for 30 d. Under LD, expression of Cm-*BBX24* remained unchanged and at a relatively high level. By contrast, under SD, where time to flowering is substantially reduced, expression substantially decreased from 3 d, and remained at a relatively low level (Supplemental Figure 2B). Thus, expression of Cm-*BBX24* is responsive to daylength.

Structural Features of Cm-BBX24

Cm-BBX24 contains two B-box domains in the N terminus and no CCT domain (Figure 2A). The B-box is a zinc binding domain, consisting of conserved Cys and His residues. To obtain supporting evidence that Cm-BBX24 functions as a transcription factor, we determined the subcellular localization of a fusion protein comprising Cm-BBX24 fused to green fluorescent protein (Cm-BBX24-GFP) following transient expression in onion epidermal cells. The Cm-BBX24-GFP fusion protein localized predominantly in the nucleus, while the GFP protein alone was detected in both cytoplasm and nucleus, as expected (Figure 2B).

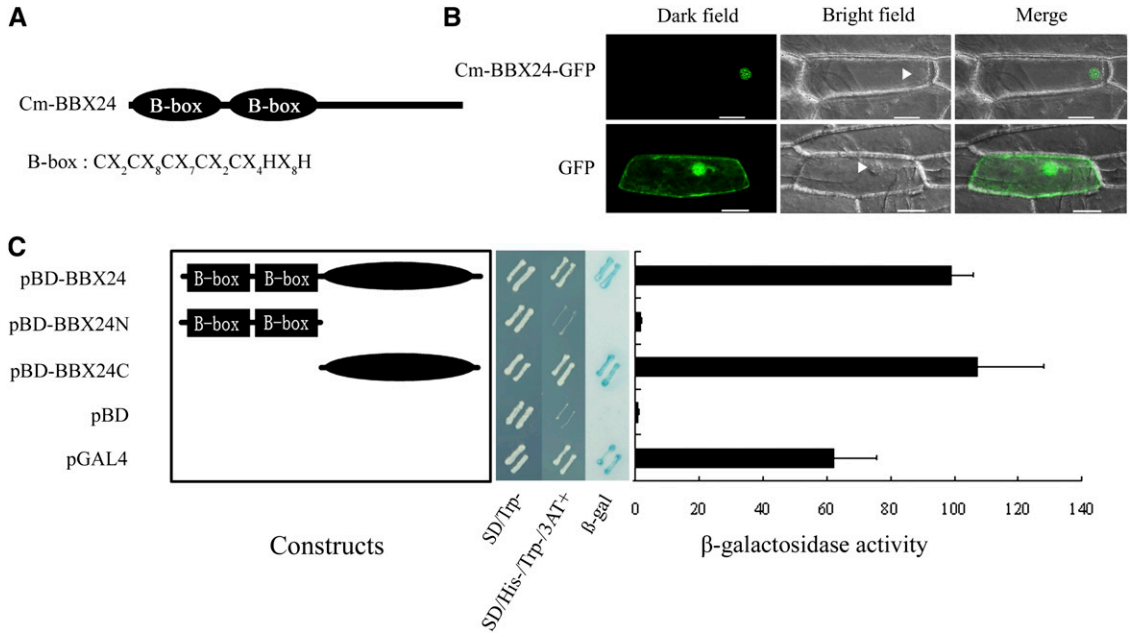

Figure 2. Protein Structure, Subcellular Localization, and Transactivation of Cm-BBX24.

(A) Schematic diagram of the protein structures.

(B) Subcellular localization in onion epidermal cells. Arrowheads indicate nuclei. Images are shown as dark field (left), bright field (middle), and merged (right). Bars = 50 μm.

(C) Transactivation activity analysis in yeast cells. Left panel: Diagram of the three different constructs of Cm-BBX24. The pBD and pGAL4 plasmids were used as the negative and positive controls, respectively. Middle panel: transactivation activity. SD-Trp, SD medium without tryptophan; SD/His-/Trp-/3AT+ medium, SD medium without histidine and tryptophan, but with 10 mM 3-AT; β-Gal, β-galactosidase activity. Right panel: Quantitative assay of β-galactosidase activity. Error bars indicate SD (n = 3).

We then performed a transactivation assay in yeast. The sequences encoding the ORF, N-terminal, and C-terminal regions of Cm-BBX24 were individually inserted into the expression vector pBD-GAL4, and each of the different constructs was transformed into the yeast strain YRG-2 containing the *His3* and *LacZ* reporter genes. The pGAL4 transcription factor and pBD vector were used as positive and negative controls, respectively. Yeast growth on the His-deficient medium, LacZ staining, and the relative quantitative assay of β-galactosidase activity (Figure 2C) indicated that Cm-BBX24 plays a role as a transcriptional activator and that the activation domain is present in the C-terminal region.

Growth and Development of Cm-*BBX24*–Overexpressing or RNA Interference–Suppressed Chrysanthemum Lines, and Cm-*BBX24* Overexpression in *Arabidopsis*

To establish whether Cm-*BBX24* plays a role in regulating flowering time, we overexpressed (OX) and suppressed (RNA interference [RNAi]) Cm-*BBX24* in chrysanthemum, obtaining 15 T0 clones of Cm-*BBX24*-OX and 11 T0 clones of Cm-*BBX24*-RNAi. We also evaluated the expression of all five members of chrysanthemum BBX structure group IV and confirmed that only Cm-*BBX24* was silenced in Cm-*BBX24-RNAi* plants (Supplemental Figure 3). We selected three representative transformants each for the Cm-*BBX24*-OX and Cm-*BBX24*-RNAi lines to assess their growth and development (Figure 3A). No obvious differences were observed in plant height, crown diameter, leaf numbers, flower diameter, and number of flowers in any of the transgenic lines, compared with the wild type. However, the time to flowering was significantly different in the Cm-*BBX24*-RNAi plants, relative to the wild-type or Cm-*BBX24*-OX plants (Figures 3B to 3D). At 55 d after transplanting, the Cm-*BBX24*-RNAi plants held under LD were already exhibiting differentiation of involucral primordia, while wild-type plants showed no such differentiation. Moreover, at 65 d after transplanting, the Cm-*BBX24*-RNAi plants showed differentiation of floret primordia, while wild-type plants had just initiated involucral primordium differentiation, and at 75 d after planting, the Cm-*BBX24*-RNAi plants had entered stage of petal primordium differentiation, while the wild-type plants were at the stage of floret primordium and floret preprimordium formation (Figure 3B). Subsequently, flower buds emerged and bloomed in

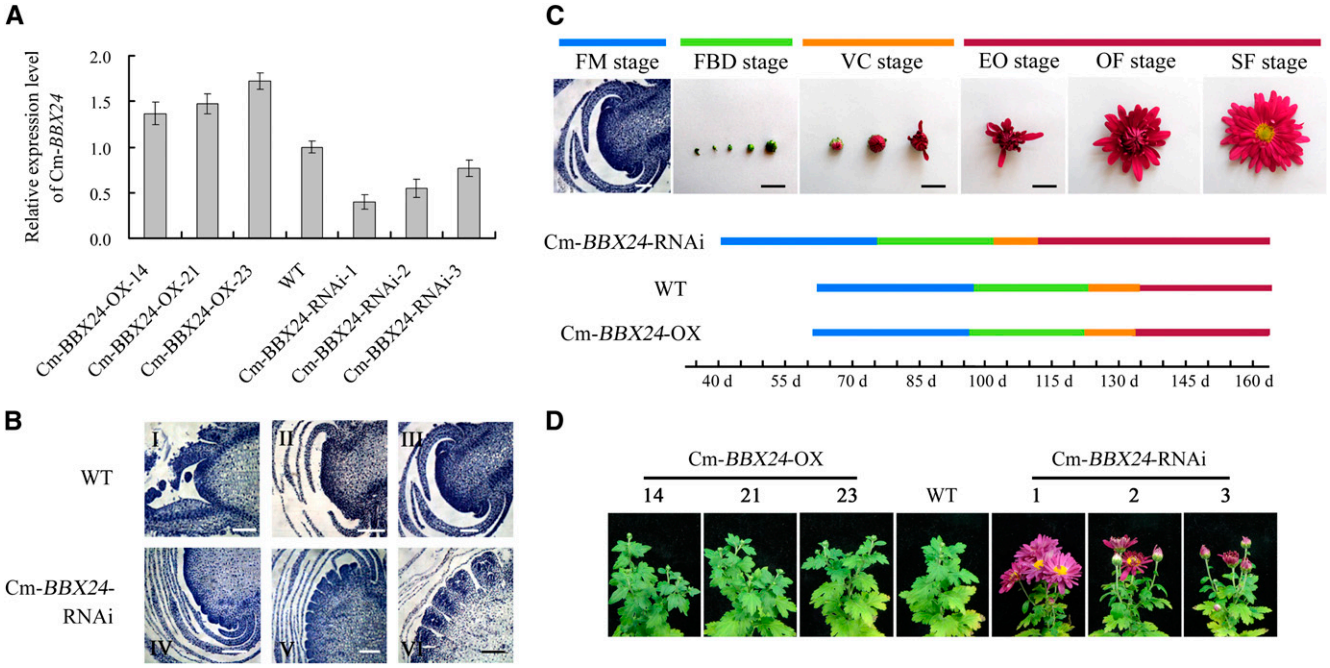

Figure 3. Phenotypic Characterization of the Cm-*BBX24*–Overexpressing (Cm-*BBX24*-OX) or RNAi-Suppressed (Cm-*BBX24*-RNAi) Chrysanthemum Plants.

(A) Expression of Cm-*BBX24* in the wild-type and transgenic plants at ZT3, determined by qRT-PCR. Cm-*BBX24*-OX-14, -21, and -23 correspond to three independent Cm-*BBX24*-OX lines, and Cm-*BBX24*-RNAi-1, -2, and -3 correspond to three independent Cm-*BBX24* RNAi lines.

(B) Inflorescence differentiation in Cm-*BBX24*-RNAi and the wild type at various stages. I, before flower bud differentiation; II, involucral primordium differentiation; III, before floret primordium differentiation; IV, involucral primordium differentiation; V, floret primordium formation; VI, petal primordium differentiation. Bars = 100 μm.

(C) Flower bud differentiation in the transgenic lines and the wild type. FM stage, floral meristem stage (bars = 100 μm); FBD stage, flower bud development stage; VC stage, visible color stage; EO stage, earlier opening stage; OF stage, opened flower stage; SF stage, senescing flower stage. Bars = 1 cm.

(D) Generative phenotype of wild-type, Cm-*BBX24*-OX, and Cm-*BBX24*-RNAi chrysanthemum lines at the reproductive stage. Plants were photographed 117 d after transplanting.

the Cm-*BBX24*-RNAi plants in advance of the wild-type plants after ~20 d. No significant difference of flowering time was observed between Cm-*BBX24*-OX and wild-type plants (Figures 3C and 3D). All of the above observations were made on plants growing under LD.

Chrysanthemum is classed as a SD-requiring plant and, as such, there might be insufficient potential to delay flowering time in Cm-*BBX24*-OX plants. To test this hypothesis, we overexpressed Cm-*BBX24* in *Arabidopsis*, which is a LD-requiring plant. Compared with *Arabidopsis* wild-type plants, Cm-*BBX24*-OX lines grown under LD showed no obvious differences in phenotypes, such as size and color rosette leaves and plant height, but there was a significant delay in flowering time, and at the bolting stage the transgenic *Arabidopsis* plants had many more rosette leaves than the control plants (Supplemental Figure 4). These results indicate that Cm-*BBX24* has the capacity to regulate flowering time in both chrysanthemum and *Arabidopsis*.

Abiotic Stress Tolerance in Cm-*BBX24*-OX and Cm-*BBX24*-RNAi Chrysanthemum

To assess the influence of Cm-*BBX24* expression on abiotic stress tolerance in chrysanthemum, we defined specific phenotypes according to the severity of the stress-induced injury. When the injury is relatively mild, the apical shoots can recover growth quickly, when the injury is moderate the apical shoots cannot recover growth, but the lateral shoots grow out instead. When the injury is severe the aerial parts die, but the basal shoots can still grow out. However, when the injury is very severe, plants cannot recover and die.

To evaluate freezing tolerance, plants were treated at −6°C for 8 h. After a subsequent 30-d recovery under normal growing conditions, wild-type plants displayed moderate damage, while almost all the Cm-*BBX24*-OX plants showed only mild damage and maintained a vigorous growth. By contrast, the Cm-*BBX24*-RNAi plants suffered serious damage (Figure 4A). In one experiment, 71% of the wild-type plants survived, with 67% depending on the outgrowth of lateral or basal shoots, i.e., there was no recovery of apical shoots. Less than 52% of the Cm-*BBX24*-RNAi plants survived, and they had weak growth, with all surviving plants depending on the outgrowth of lateral or basal shoots. However, more than 88% of the Cm-*BBX24*-OX plants survived and exhibited strong growth, and plants from Cm-*BBX24*-OX line 23 recovered with continued apical shoot formation (Figures 4A and 4B).

In the drought stress tolerance test, involving 23 d without watering followed by a 30-d recovery period, almost all the Cm-*BBX24*-OX plants showed mild damage with subsequent vigorous growth, while the Cm-*BBX24*-RNAi plants were seriously damaged. In one experiment, 54% of wild-type plants survived, but for the Cm-*BBX24*-RNAi plants, survival rate was only 39%, and almost all of the surviving plants showed only weak outgrowth of the lateral or basal shoots. However, more than 77% of the Cm-*BBX24*-OX plants survived, and half of those plants recovered quickly with continuous growth of their apical shoots (Figures 4A and 4B).

For the salt stress tolerance study, plants were treated with NaCl for 28 d, after which time all the leaves displayed symptoms of damage, with no obvious differences being observed between the wild-type, Cm-*BBX24*-RNAi, and Cm-*BBX24*-OX plants (Figure 4A).

Collectively, these results provide evidence that Cm-*BBX24* overexpression can enhance tolerance by chrysanthemum of both low temperatures and drought. By contrast, there was no evidence of improved tolerance to salt stress.

Global Expression Analysis of Cm-*BBX24* Downstream-Associated Transcripts Related to Flowering Time and Abiotic Stress Tolerance

To better understand the regulatory mechanisms of Cm-*BBX24*–mediated regulation of flowering time and abiotic stress tolerance, we performed a large-scale screen of genes that are differentially expressed between wild-type and Cm-*BBX24*-OX or RNAi chrysanthemum plants using an RNA sequencing (RNA-seq) approach. The raw sequence reads were deposited into the National Center for Biotechnology Information SRA database under the accession numbers SRP038981 and SRA091277. The assembled transcripts that were differentially expressed in Cm-*BBX24* transgenic chrysanthemum plants are listed in Supplemental Data Set 1.

In the context of the regulation of flowering time by Cm-*BBX24*, we focused on the transcripts that were differentially expressed between Cm-*BBX24*-RNAi and wild-type plants. Based on their annotation, we selected nine transcripts that were upregulated 2-fold and seven that were upregulated 1.5-fold in Cm-*BBX24*-RNAi plants compared with wild-type plants (Supplemental Figure 5). The corresponding genes are predicted to be components of the photoperiod pathway, GA biosynthesis genes, GA signaling–related genes, MADS box transcription factors, etc. (Table 1). Of these genes, *PRR5*, *GI*, and *CO* (*COL*) encode proteins related to the photoperiod pathway, while the genes associated with the GA pathway are predicted to play a role in biosynthesis or signal transduction, such as those encoding GA3-oxidase, GA20-oxidase, gibberellin-regulated protein (GRP), GRAS, and flowering promoting factor-like 1 (FPF1). We also observed that *FT* and *SOC1*, which are known flowering integrators, were differentially expressed between Cm-*BBX24*-RNAi and wild-type chrysanthemum lines (Table 1). Collectively, the expression data suggest that Cm-*BBX24* effects on flowering time may occur by influencing the regulation of expression for genes that are related to both the photoperiod and GA pathways.

In terms of abiotic stress tolerance, we focused on transcripts that were upregulated in Cm-*BBX24*-OX plants but downregulated in Cm-*BBX24*-RNAi plants, both relative to wild-type chrysanthemum. Of the 43 assembled transcripts in this category, 36 have functional annotations based on sequence similarity, while seven have no assigned function (Supplemental Figure 5). The putative proteins corresponding to the assembled transcripts were further classified into two groups: regulatory proteins and functional proteins (Supplemental Table 1). The former category includes five predicted transcription factors (e.g., WRKY and MYB), two signaling proteins (e.g., calmodulin), and four protein kinases (e.g., a receptor kinase). We note that most of these classes of proteins have previously been reported as being stress responsive (Seki et al., 2002). The category of functional proteins includes LEA and dehydration response

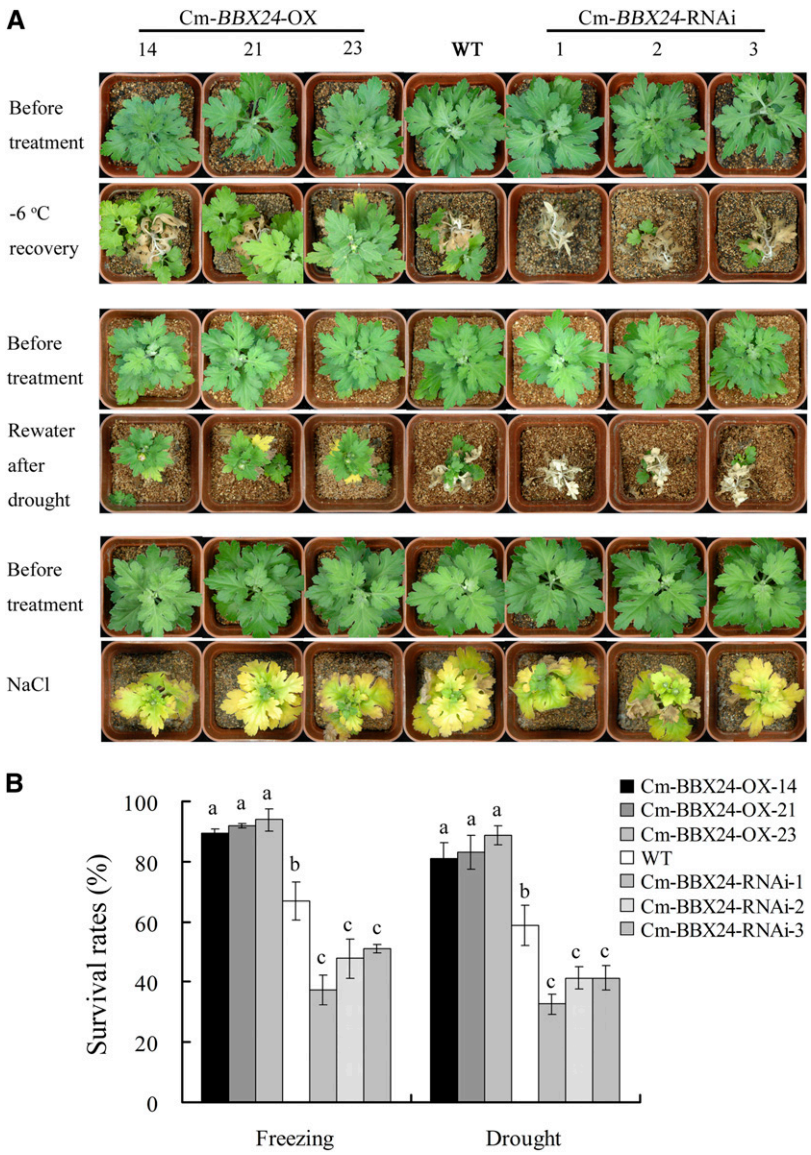

Figure 4. Abiotic Stress Tolerance of Cm-*BBX24*-OX and Cm-*BBX24*-RNAi Chrysanthemum Lines.

(A) Abiotic stress tolerance of Cm-*BBX24*-OX and Cm-*BBX24*-RNAi lines. Cm-*BBX24*-OX-14, -21, and -23 are three independent T0 lines, as are Cm-*BBX24*-RNAi-1, -2, and -3.

(B) The survival rates of Cm-*BBX24*-OX and Cm-*BBX24*-RNAi lines grown under abiotic stress conditions. Three independent experiments were performed and error bars indicate SD. Significant differences were determined by Duncan's multiple range test ($P < 0.05$).

proteins, compatible solute-related proteins (e.g., lectins), carbohydrate metabolism–related proteins (e.g., UDP-glycosyltransferase), and oxidation-reduction process-related proteins (e.g., cytochrome oxidase subunit). These proteins have also previously been reported to act either directly or indirectly in abiotic stress responses (Seki et al., 2002).

To validate the data from the RNA-seq digital expression analysis, we performed qRT-PCR assays of seven abiotic response- and flowering time–related genes. The results showed that although there were some anomalous quantitative differences, the trends of gene expression changes detected by the two different approaches were generally consistent (Supplemental Table 2), thereby confirming the validity of the RNA-seq data.

Involvement of GAs in Cm-*BBX24*–Influenced Flowering Time and Abiotic Stress Tolerance

As described above, some of the transcripts related to GA biosynthesis genes and GA signaling genes were downregulated in the Cm-*BBX24*-OX lines and upregulated in Cm-*BBX24*-RNAi lines (Table 1). The qRT-PCR analyses confirmed that expression of *GA20ox* and *GA3ox* was increased to 3.34- and 2.92-fold in

Table 1. Upregulated Transcripts Related to Flowering Time in Cm-*BBX24*-RNAi Plants

Gene	Annotation	Fold Change	
		OX/WT	RNAi/WT
Photoperiod pathway			
UN052290	GIGANTEA	1.14	1.62
UN055998	GIGANTEA	0.95	1.53
UN005597	PRR5	0.65	1.88
UN052854	CONSTANS	1.02	2.11
UN064661	CONSTANS-like	0.73	1.70
GA biosynthesis and signaling			
UN031599	Gibberellin 20-oxidase	0.19	3.38
UN049353	Gibberellin 3-oxidase2	0.62	2.71
UN035573	GRP	1.05	2.01
UN030255	GAI, RGA, and SCARECROW (GRAS)	1.37	2.99
UN052024	FPF1	1.68	3.56
Flowering integrators			
UN060780	SOC1	1.07	1.61
UN052931	FT	1.14	1.51
MADS box genes			
UN014190	MADS box transcription factor CDM111	1.04	13.00
UN001497	MIKC MADS box transcription factor	1.75	7.60
UN059046	MADS box transcription factor CDM41	0.68	1.83
AP2-EREBP genes			
UN033682	Transcription factor AP2-EREBP	0.33	11.64

Significant differences were determined with $P < 0.05$ and expression ratio ≥ 1.5. WT, the wild type.

Cm-*BBX24* transgenic chrysanthemum plants relative to expression levels seen for wild-type plants (Supplemental Table 2). We also determined expression of genes related to GA biosynthesis, including *GA20ox* (*1* to *5*), *GA3ox* (*1* and *2*), and *GA2ox* (*GA 2-oxidases*) (*1* to *4*, *6*, and *7*) in Cm-*BBX24*-OX *Arabidopsis* plants. Relative to wild-type plants, expression of *GA20ox2* and *GA3ox1* was clearly downregulated in Cm-*BBX24*-OX *Arabidopsis*, whereas expression of all the *GA2ox* genes tested showed no differences (Supplemental Figures 6A and 6B).

We then quantified the levels of endogenous GAs in young leaves of the transgenic chrysanthemum lines and compared these GA levels to those found for wild-type plants grown under different daylengths. As a general tendency, bioactive GA_1 was much more abundant than GA_4 in both transgenic and wild-type plants under either LD or SD (Table 2). Under LD, the Cm-*BBX24*-RNAi plants had concentrations of GA_1 and GA_4 that were 2.3 and 1.8 times greater, respectively, than levels found for wild-type plant leaves. For GA_{19} and GA_{20}, which are precursors of GA_1, their levels in young leaves were 2.1 and 1.5 times greater than found for the wild type (Table 2). Other GAs quantified by the stable isotope dilution method either showed no changes or were not detectable. Under SD, GA_1 and GA_4 increased slightly, relative to wild-type young leaves, but no obvious changes in GA_{19} and GA_{20} levels were apparent in Cm-*BBX24*-RNAi plants compared with wild-type plants (Table 2). For Cm-*BBX24*-OX plants compared with the wild type, of the GAs detected, GA_1 and GA_4 contents showed a substantial decrease under LD, though these two bioactive GAs remained relatively high under SD (Table 2). These results suggest that Cm-*BBX24* expression results in changes in the steady state levels of GA_4 and GA_1 concentrations

Table 2. Concentration of GAs in the Leaves of Cm-*BBX24*-OX/RNAi and Wild-Type Chrysanthemum Lines under SD and LD

Daylength	Lines	GA Content ($ng \cdot g^{-1}$ FW)						
		GA_1	GA_4	GA_{19}	GA_{24}	GA_{20}	GA_3	GA_8
SD	Cm-*BBX24*-RNAi	1.73 ± 0.17 a	0.33 ± 0.04 a	1.10 ± 0.16 a	0.31 ± 0.07 a	0.35 ± 0.03 a	0.34 ± 0.05 a	0.80 ± 0.23 a
	Wild type	1.64 ± 0.19 a	0.22 ± 0.05 b	0.94 ± 0.17 a	0.29 ± 0.05 a	0.36 ± 0.09 a	0.38 ± 0.09 a	0.60 ± 0.06 a
	Cm-*BBX24*-OX	1.46 ± 0.13 a	0.23 ± 0.04 b	1.02 ± 0.14 a	0.21 ± 0.06 a	0.37 ± 0.06 a	0.42 ± 0.09 a	0.56 ± 0.23 a
LD	Cm-*BBX24*-RNAi	1.45 ± 0.26 a	0.34 ± 0.03 a	1.40 ± 0.04 a	nd	0.43 ± 0.04 a	0.21 ± 0.03 a	1.04 ± 0.34 a
	Wild type	0.62 ± 0.11 b	0.18 ± 0.01 b	0.67 ± 0.07 b	nd	0.28 ± 0.07 b	0.19 ± 0.04 a	0.69 ± 0.18 a
	Cm-*BBX24*-OX	0.37 ± 0.08 c	0.12 ± 0.01 c	0.58 ± 0.05 b	nd	0.32 ± 0.02 b	0.20 ± 0.02 a	0.94 ± 0.07 a

Cm-*BBX24*-OX, the wild type, Cm-B*BX24*-RNAi, and three different chrysanthemum lines. SD, 8-h SD; LD, 16-h LD. Significant differences were determined by Duncan's multiple range test ($P < 0.05$, $n = 3$), and lowercase letters, a to c, indicate significant differences between wild-type and transgenic plants under SD or LD condition. nd, endogenous GA not detected, deuterated GA internal standard present. GA_5, GA_9, GA_{29}, GA_{34}, and GA_{51} were not detected.

in the young leaves, and notably the two precursors of GA_1, GA_{19}, and GA_{20} also showed similar increases. It should be noted, though, that these changes in GA concentration in the young leaves occurred only under LD, where flowering is appreciably delayed.

To establish whether Cm-BBX24 influences the floral integrator through the GA pathway, we determined expression patterns of Cm-*BBX24* and five chrysanthemum *FT* genes with $GA_{4/7}$ applications under the two different daylengths. The five *FT* genes were identified by querying our chrysanthemum RNA-seq database (Table 1), as well as data presented in a recent publication (Higuchi et al., 2013). Cm-*BBX24* expression changed in response to daylength, and the expression patterns were consistent with that of the antiflorigen (e.g., Cm-*AFT*), and opposite from those of florigen (e.g. Cm-*FTL3*) under both SD and LD (Figure 5A). Exogenously applied $GA_{4/7}$ suppressed the expression of Cm-*BBX24* under either LD or SD, whereas the expression of the five Cm-*FTs* showed varying patterns in response to the $GA_{4/7}$ treatment. We note that clear suppression of Cm-*BBX24* expression by the GA treatment is consistent with that of antiflorigen (e.g., Cm-*AFT*) but is opposite to that of florigen (e.g., Cm-*FTL3* and Cm-*TFL1*) under LD (Figure 5A). It should also be noted that applied bioactive GAs act as potent florigens in chrysanthemum, both in this study (Figure 5A) as well as in a previous study (Pharis, 1972).

We then analyzed the consequences of Cm-*BBX24* suppression on the expression patterns of flowering-time integrators in chrysanthemum. Under either LD or SD, expression of Cm-*FTL3* and Cm-*SOC1* was much higher in the Cm-*BBX24*-RNAi lines

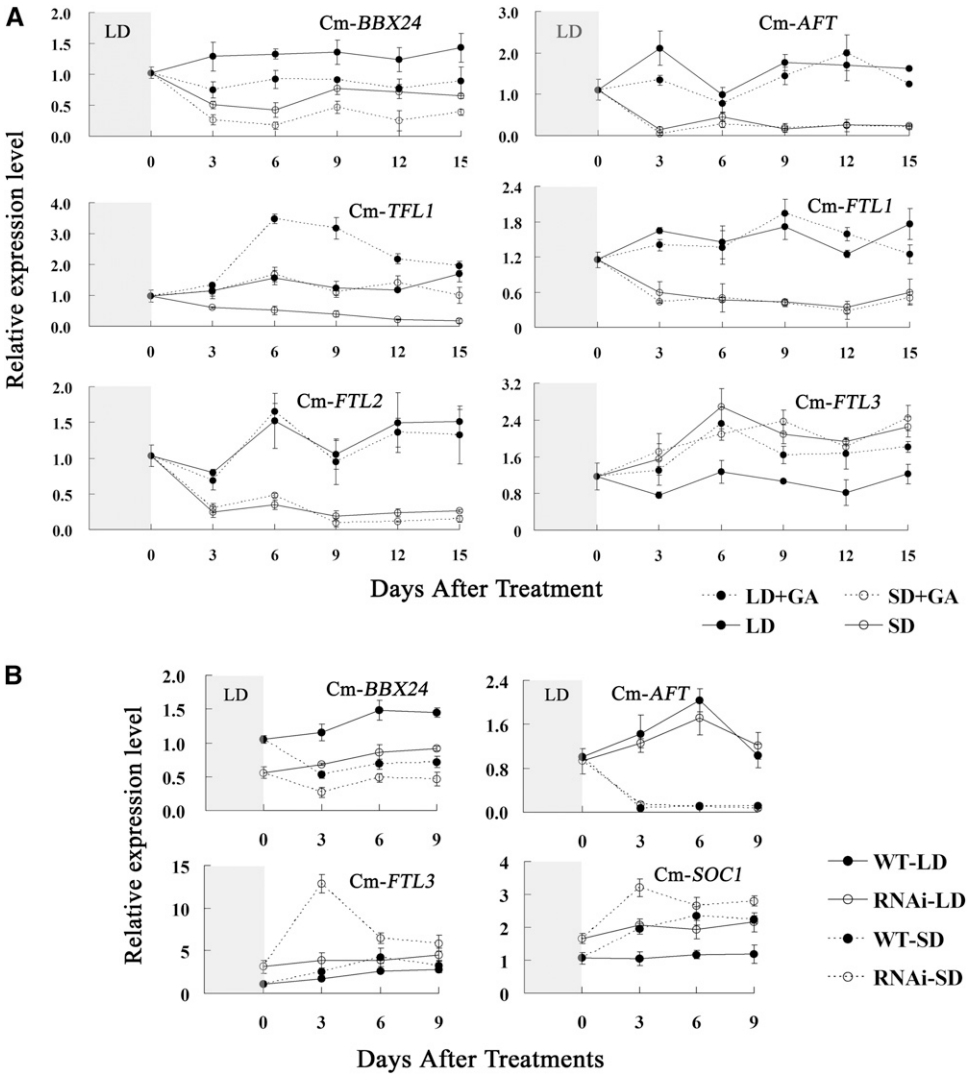

Figure 5. Expression Profiles of Cm-*BBX24* and Flowering-Time Integrators under Different Daylengths or following $GA_{4/7}$ Applications for Chrysanthemum Plants.

(A) Expression profiles of Cm-*BBX24* and Cm-*FTs* under different daylengths or following $GA_{4/7}$ treatments. The gray area indicates LD, and 0 indicates the time at which the plants were transferred to SD. The data were normalized with *Ubiquitin* expression. Error bars indicate SD (n = 3).

(B) Expression profiles of Cm-*BBX24* and flowering-time integrators under different daylengths in Cm-*BBX24*-RNAi plants. RNAi, Cm-*BBX24*-RNAi.

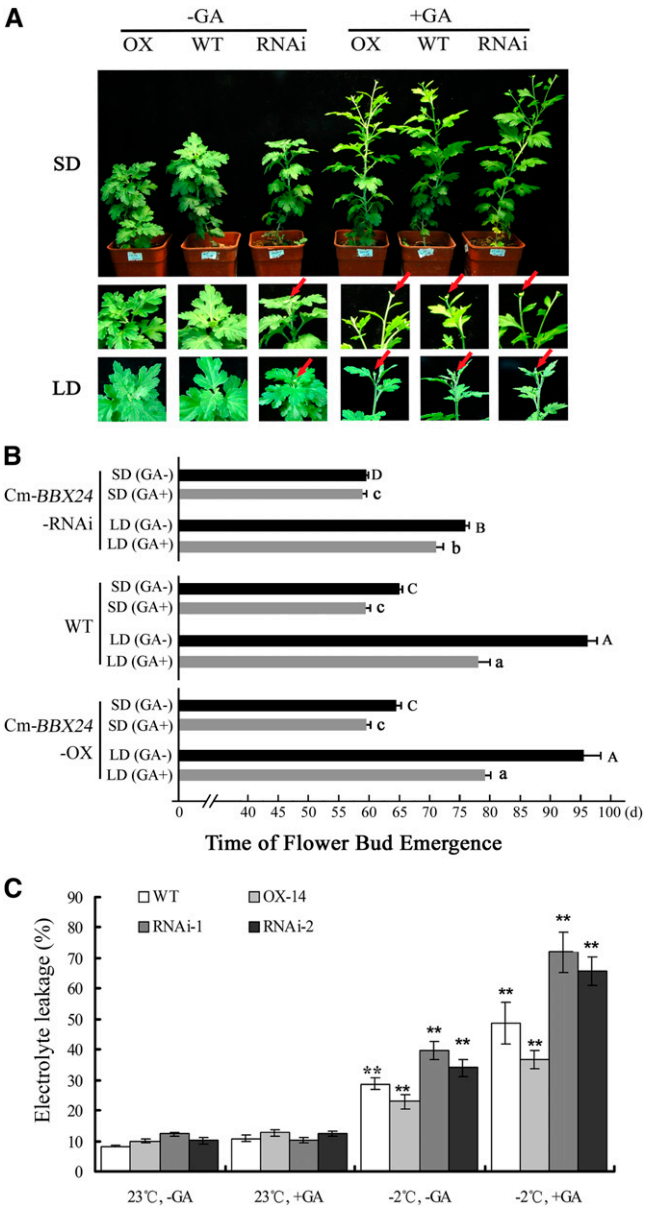

Figure 6. Effect of $GA_{4/7}$ Treatment on Flowering Time and Electrolyte Leakage in Transgenic Cm-*BBX24* Chrysanthemum Plants.

(A) Flower bud emergence of wild-type and Cm-*BBX24*-OX/RNAi chrysanthemum plants treated with $GA_{4/7}$ under LD or SD. The plants were photographed 65 and 85 d after transplanting under SD and LD, respectively. Red arrows indicate the emergence of visible flower buds.

(B) Effect of $GA_{4/7}$ application on flower bud emergence time in wild-type and Cm-*BBX24*-OX/RNAi transgenic chrysanthemum lines. The columns indicate the duration of the vegetative growth period of different plants with or without $GA_{4/7}$ treatments under LD or SD. 0 d represents the transplanting time, and GA treatment was performed at 30 d. Three independent experiments were performed, and error bars indicate SD (n = 3). Significant differences were determined by Duncan's multiple range test ($P < 0.05$), and capital letters (A to D) and small letters (a to c) indicate significant differences in comparisons among control plants (no $GA_{4/7}$ treatment) and plant given the $GA_{4/7}$ spray treatments, respectively.

(C) Effect of $GA_{4/7}$ treatment on electrolyte leakage of chrysanthemum. OX-14, a line of Cm-*BBX24*-OX; RNAi-1 and RNAi-2, two independent lines of Cm-*BBX24-RNA*i. 23°C, -GA (normal growth conditions); 23°C, +GA (normal growth conditions with an exogenous $GA_{4/7}$); -2°C -GA (freezing treatment); -2°C +GA (freezing with an exogenous $GA_{4/7}$). Three independent experiments were performed, and error bars indicate SD (n = 3). Significant differences were determined by Duncan's multiple range test ($P < 0.05$), and asterisks indicate significant differences in comparisons among control plants (no $GA_{4/7}$ treatment) or plants given the $GA_{4/7}$ spray treatments.

than in wild-type plants, whereas expression of Cm-*AFT* showed essentially no difference (Figure 5B). We also evaluated the expression of potential target genes of Cm-BBX24, including *GI*, *CO*, *FT*, and *SOC1* in the *Arabidopsis* Cm-*BBX24* transgenic plants. Relative to wild-type plants, expression of all the tested genes related to the photoperiod pathway was clearly downregulated in Cm-*BBX24*-OX *Arabidopsis* (Supplemental Figure 6A).

We further tested the effect of exogenous $GA_{4/7}$ on flowering time of chrysanthemum. In one experiment under LD, without GA treatment, the blossom time was 76 and 96 d in Cm-*BBX24*-RNAi and wild-type plants, respectively, a 20-d advance in flowering time. With $GA_{4/7}$ treatment, the flowering time was 72 and 78 d in Cm-*BBX24*-RNAi and wild-type plants, respectively, an advance of only 6 d by the transgenic line under LD, though an 18-d advance was seen for the wild type. Under SD, the $GA_{4/7}$ applications yielded a flowering time for all three genotypes that was approximately the same (Figures 6A and 6B). $GA_{4/7}$ application to the Cm-*BBX24*-OX *Arabidopsis* plants under LD rescued the late-flowering phenotype of the transgenic line, but there was no significant difference in leaf numbers between the transgenic and wild-type plants (Supplemental Figures 6D and 6E). These results indicate that the $GA_{4/7}$ treatment countered the suppressing effect of Cm-*BBX24* overexpression.

Together, these results suggest that Cm-*BBX24* influences flowering, at least in part, via the GA pathway under LD, i.e., under a daylength where flowering is appreciably delayed.

Changes in GA biosynthesis are known to be associated with abiotic stress responses in some plant species (Achard et al., 2008). Here, Cm-*BBX24* transgenic chrysanthemum lines, relative to wild-type plants, showed clear changes in expression of several GA biosynthesis genes (*GA20ox* and *GA3ox*) and in young leaf GA concentration (Tables 1 and 2). However, the expression levels of *GA2ox* and concentration of GA_8, the product of GA2ox activity, showed no apparent difference (Supplemental Figure 6C; Table 2). Therefore, we speculate that changed abiotic stress tolerance in Cm-*BBX24* transgenic plants may be related to the influence of increased levels of bioactive GAs, rather than by not inactivation via GA2ox action.

To further investigate the speculation, we tested the influence on cold tolerance of $GA_{4/7}$ applied to young chrysanthemum leaves. Under normal temperatures, $GA_{4/7}$ treatment had no effect on electrolyte leakage, but following a −2°C low-temperature treatment, the electrolyte leakage of all plants increased significantly, and the $GA_{4/7}$ treatment exacerbated the low temperature-induced damage: The $GA_{4/7}$ treatment increased leakage by 70% in wild-type plants, but only 59% in Cm-*BBX24*-OX plants. By contrast, electrolyte leakage was 82 and 93% in the two Cm-*BBX24*-RNAi

lines. Thus, exogenously applied $GA_{4/7}$ reduced the tolerance to low temperatures and did so particularly for the Cm-*BBX24*-RNAi transgenic plants (Figure 6C).

DISCUSSION

Involvement of Cm-*BBX24* in the Regulation of Flowering Time

It has been established that *CO* encodes a putative zinc finger transcription factor and that its temporal and spatial regulation is key to the daylength-dependent induction or promotion of flowering (Putterill et al., 1995). In terms of the relationship between the structures and functions of BBX proteins, a previous analysis of seven *Arabidopsis co* mutant alleles demonstrated that mutations within either the B-box region or the CCT domain influence flowering time, underlining the importance of these two conserved regions in the regulation of flowering time by CO (Robson et al., 2001). However, it is worth noting that *BBX32*, a member of structure group V, and some *COLs* (*COL6-8*, *16/BBX14-17*), belonging to structure group III, can also influence flowering time, even though they encode proteins with just a single B-box domain. In this study we demonstrate that chrysanthemum BBX24, a member of structure group IV, influences flowering time, even though it does not contain a CCT domain. Collectively, our data suggest that the first B-box domain in the BBX proteins plays a causal role in influencing flowering time.

As components of the photoperiod pathway, *GI*, *PRR5*, *CO*, *FT*, and *SOC1* are thought to be important in the control of flowering time. For example, *GI* is an essential component of the daylength control of flowering, and in *Arabidopsis*, *gi* mutants show a late-flowering phenotype and reduced accumulation of *CO* transcripts (Fowler et al., 1999). In this study, we used RNA-seq-based transcript profiling to show that the expression levels of a range of genes with homology to known components of flowering regulatory pathways, including *GI*, *PRR5*, *CO*, *FT*, and *SOC1*, were upregulated in Cm-*BBX24*-RNAi transgenic chrysanthemum, relative to wild-type plants (Table 1). These findings suggest that Cm-*BBX24* influences flowering time in part by modulating the photoperiod-induced pathway at the transcriptional level.

GA biosynthesis genes and GA downstream-signaling responses are involved in the regulation of flowering time (Mouradov et al., 2002). The GA3ox protein catalyzes the conversion of precursor 3-deoxy GAs to their bioactive forms and therefore plays a direct role~~s~~ in determining the levels of bioactive GAs in plants (Pimenta Lange and Lange, 2006). However, the bioactive GA_1 and GA_4 can be deactivated through oxidation by GA2ox to the inactive GA_{34} and GA_8, respectively, and GA2ox may also play a regulatory role in determining bioactive GA levels (Hedden and Phillips, 2000; Eriksson et al., 2006). In addition, GRP, an important component of the GA signaling pathway, has been reported to participate in regulating flowering time in *Arabidopsis* (Zhang et al., 2009). *GRAS* genes also function in GA signal transduction and thus can play a role in regulation of flowering (Dill and Sun, 2001). Additionally, the FPF1 functions in the GA-dependent signaling pathway in *Arabidopsis* (Kania et al., 1997).

Chrysanthemum, a SD-requiring plant, has long been used as a model in classical physiological experiments to study the effect of daylength and low-temperature vernalization on flowering. In its natural setting, chrysanthemum flower bud initiation occurs eventually in all cultivars, even when grown in LD, but this may take many months in unvernalized shoots of cold-requiring cultivars (Cockshull, 1985). Flowering time of chrysanthemum is also influenced by several plant hormones (Cockshull, 1985), and among them GAs have been documented as promoting chrysanthemum flowering under LD (Pharis, 1972; Sumitomo et al., 2009). In this study, the Cm-*BBX24*-RNAi chrysanthemum clearly exhibited early flowering in LD, and RNA-seq analyses revealed that some key GA biosynthesis genes, such as *GA20ox* and *GA3ox*, as well as those genes associated with downstream GA signaling, such as a *GRP*, *GRAS*, and *FPF1*, were upregulated in Cm-*BBX24*-RNAi plants, relative to wild-type plants (Table 1).

The influence of GAs on flowering time depends on daylength. For LD-requiring plants, such as the 'Ceres' cultivar of the grass *L. temulentum*, GAs are the only plant hormones known to substitute for the single LD required for flowering (Evans and King, 1985). In *L. temulentum*, GA_5 is the primary LD-induced flowering stimulus with GA_1 and GA_4 being secondary, late-acting LD stimuli for inflorescence differentiation. Gibberellin A_6 is also a LD-induced florigenic GA (King et al., 2001, 2003; reviewed in King, 2012). In the LD-requiring *Arabidopsis*, GA_4 is the key bioactive GA in both growth and (likely) the regulation of flowering (Eriksson et al., 2006). Applied GAs have a long history of being able to replace the LD requirement and can also substitute for low temperatures in some cold-requiring plants (Pharis and King, 1985). Additionally, overexpression of *GA20ox* or GA_3 application can promote early flowering in *Arabidopsis* (Coles et al., 1999). Studies with spinach (*Spinacia oleracea*) further revealed that GA_{53}, a precursor of GA_{19}, is converted only to GA_{19} in noninductive SD, but is rapidly converted to GA_{20} when plants are transferred from SD to LD (reviewed in Pharis and King, 1985). It seems likely that LD-induced changes in *GA20ox* expression are involved in these conversion processes (Olszewski et al., 2002).

In chrysanthemum, inflorescence development (flowering) can eventually occur under noninductive LD, and exogenous application of GA_3, $GA_{4/7}$, or a combination of GA_5 with the cytokinin benzyladenine can appreciably shorten the time to flowering, with GA concentration being a limiting factor for inflorescence development and the GA_5 plus benzyladenine treatment having the strongest effect (Pharis, 1972). We also observed that suppression of Cm-*BBX24* significantly increased the levels of both bioactive GA_1 and GA_4, as well as the concentration of GA_{19} and GA_{20} (Table 2), and that these changes in endogenous GA concentration were more apparent under LD than SD. Additionally, $GA_{4/7}$ application rescued the early flowering phenotype of chrysanthemum that was created by a reduction in Cm-*BBX24* expression (Figure 6). We therefore hypothesize that under LD, the observed earlier flowering in Cm-*BBX24*-RNAi chrysanthemum lines is partially due to an increase in steady state levels of bioactive GA_1 and GA_4, the former involving the $GA_{19} \rightarrow GA_{20} \rightarrow GA_1$ pathway.

We noted that compared with wild-type plants, *BBX24*-OX chrysanthemum lines did not exhibit delayed flowering, whereas a delay was seen when Cm-*BBX24* was overexpressed in *Arabidopsis* (Supplemental Figure 4). Nevertheless, possible target

genes of Cm-*BBX24* related to GA biosynthesis pathways were clearly downregulated in Cm-*BBX24*-OX transgenic *Arabidopsis*, relative to the wild-type controls (Supplemental Figure 6B). Thus, we postulate that Cm-*BBX24* acts, under LD, by regulating GA biosynthesis and/or signaling pathways.

FT and SOC1 are known as integrators of photoperiodic and GA pathways (Moon et al., 2003; Song et al., 2013). For the LD plant *L. temulentum*, the regulation of floral apex induction appears to be mediated by LD-induced changes in endogenous GA_5 (and possible also GA_6) in the apex, as well as by *FT* (King et al., 2006). In *Arabidopsis*, flowering under noninductive SD also appears to be GA dependent, as treatment with exogenous GAs activates the transcription of *SOC1* and *LFY* (Blázquez et al., 1998; Moon et al., 2003).

For chrysanthemum, a SD plant, responses of different *FT* genes to daylength differed. *FTL3* is a key regulator of the photoperiodic flowering pathway in chrysanthemum (Oda et al., 2012) and Cs-FTL3 signaling from the leaves to the shoot tip has been reported to be affected by environmental factors, including high temperature (Nakano et al., 2013). In addition, a recent analysis revealed that the gated induction system of a systemic floral inhibitor, Cs-ATF1, an antiflorigen, determines obligate SD flowering in chrysanthemum (Higuchi et al., 2013).

In this study, we characterized the expression patterns of Cm-*BBX24* and five *FT* genes and performed a correlation analysis with daylength and $GA_{4/7}$ treatment of chrysanthemum. Our results indicated that Cm-*BBX24* is expressed at high levels under LD and was suppressed by $GA_{4/7}$ application. Furthermore, the expression patterns of Cm-*BBX24* are consistent with that of the antiflorigen (Cm-*AFT*). In addition, silencing of Cm-*BBX24* in chrysanthemum clearly induced expression levels of Cm-*FTL3* and Cm-*SOC1* (Figure 5B). We therefore propose that Cm-*BBX24* suppresses flowering by influencing both the photoperiod and GA pathways and that under LD it is Cm-BBX24 that modulates flowering, mainly through effects on the GA pathway.

Involvement of Cm-*BBX24* in the Regulation of Abiotic Stress Tolerance

Since we determined that Cm-*BBX24* expression can confer abiotic stress tolerance, especially to drought and freezing, we focused on the possible downstream genes that are upregulated in Cm-*BBX24*-OX lines, but downregulated in Cm-*BBX24*-RNAi lines. Among the 36 assembled annotated transcripts that fell into this category, seven encode regulatory proteins, including members of the WRKY, MYB, and zinc finger families, which are known to function as part of a large regulatory network that senses and responds to different environmental stimuli (Hirayama and Shinozaki, 2010). In addition, two transcripts encode proteins that are related to signaling mediated by calcium ions, which are regarded as important secondary messengers in eliciting responses to abiotic stresses (Kader and Lindberg, 2010). In addition, among the five genes encoding protein kinases, a receptor-like protein kinase was identified, a homolog of which was previously reported to be stress inducible (Hong et al., 1997).

The group of differentially expressed genes also includes those annotated as encoding functional proteins. One subset comprises proteins associated with compatible solutes, such as lectins and a homolog of tuber agglutinin. Lectins are carbohydrate binding proteins that specifically recognize diverse sugar structures and can participate in abiotic stress regulation (Jiang et al., 2010). A second group comprises genes encoding carbohydrate metabolism-related proteins. Of these, trehalose-6-phosphate synthase, UDP-glucose glucosyltransferase, and β-amylases have been reported to be regulated by drought, cold, or high-salinity stress (Seki et al., 2002), and drought stress can increase β-amylase activity (Todaka et al., 2000). Overexpression of the *Arabidopsis TREHALOSE-6-PHOSPHATE SYNTHASE* (*TPS*) gene conferred dehydration tolerance and delayed flower development in transgenic plants (Avonce et al., 2004), and overexpression of the yeast *TPS* gene improved tolerance to abiotic stresses in tomato (*Solanum lycopersicum*) (Cortina and Culianez-Macia, 2005), suggesting that these genes play similar roles in chrysanthemum.

In terms of correlations between GA biosynthesis and abiotic stress tolerance, it has been reported that overexpression of an endogenous *GA20ox* in citrus plants resulted in increased of GA content and thus decreased in abiotic stress tolerance (Huerta et al., 2008). This was accompanied by global upregulation of genes involved in photosynthetic and carbon utilization, downregulation of genes associated with protein biosynthesis and ribosome biogenesis, and the differential expression of numerous genes related to abiotic stress responses (Huerta et al., 2008). In *Arabidopsis*, endogenous GA_4 content of the shoot is negatively correlated with expression of *CBF1/DREB1b*, and elevated *CBF* expression reduces the accumulation of bioactive GAs through expression levels of *GA2ox* in cold-induced plants (Achard et al., 2008). CBFs are considered to function as integrators of phytochrome and GA signaling during cold acclimation, and such integration can lead to the activation of the *CBF* regulon and subsequent upregulation of *COR* gene and *GA2ox* expression, the latter resulting in a dwarf phenotype, coupled with increased freezing tolerance and enhanced photosynthetic performance (Kurepin et al., 2013).

In this study, we also noted that under LD, *GA20ox* and *GA3ox* were significantly upregulated in Cm-*BBX24*-RNAi transgenic lines and significantly downregulated in Cm-*BBX24*-OX lines, both relative to wild-type chrysanthemum (Supplemental Table 2). By contrast, *GA2ox* showed no difference in expression in our transgenic lines (Supplemental Figure 6C). These results suggest that Cm-BBX24 regulates bioactive GA levels mainly through influencing GA biosynthesis rather than inactivation. Therefore, we propose that Cm-*BBX24* acts independently of *CBF1/DREB1b*.

It has been reported that some flowering-associated genes function to regulate flowering time and are also involved in the abiotic stress response. *GI*, a circadian clock gene, is induced by cold stress and appears to be involved in mediating the cold stress response, possibly by positively regulating freezing tolerance via a CBF-independent pathway (Cao et al., 2005). Plants with loss-of-function mutations in *GI* and *CO* exhibited abnormal drought-escape phenotypes. The peak mRNA levels of *GI* and *Flavin binding Kelch domain F box protein 1* and the mRNA levels of *CO* and *FT* were shown to change under drought stress (Han et al., 2013). *Pseudo-RRs* (*PRRs*), clock-associated genes that regulate flowering time positively, are also implicated in abiotic stress responses, where they function as negative regulators

(Nakamichi et al., 2009). In *Arabidopsis*, a decreased level of *SOC1* results in derepression of cold-inducible genes, which appears to enable plants to respond more effectively to low temperature stress (Seo et al., 2009). In *Pharbitis nil*, the expression of *FT2*, one of two homologs of the floral pathway integrator gene, *FT*, was induced by low temperature (Yamada and Takeno, 2014).

Our results imply that Cm-*BBX24* may be an important regulator of the crosstalk between flowering time and abiotic stress responses regulation in chrysanthemum. If so, the ability to influence flowering time and abiotic stress responses via the same set of genes may provide an evolutionary advantage.

In summary, Cm-*BBX24* encodes a zinc finger transcription factor that may play a pivotal role in flowering time regulation and abiotic stress responses. Cm-*BBX24* possibly acts as a repressor of flowering by negatively regulating the expression of the photoperiod flowering pathway genes *GI*, *PRR5*, *CO*, *FT*, and *SOC1*, as well as the GA biosynthesis genes *GA20ox* and *GA3ox*. It also appears to be involved in regulating the response of plants to two abiotic stresses by influencing a subset of genes that mediate stress responses and GA biosynthesis (Supplemental Figure 7). Our results suggest a conserved mechanism for regulating flowering time and abiotic stress responses in plants, and we propose that the regulation of Cm-*BBX24* may be a common feature in these two distinct responses. Future investigation to determine a more precise mechanism by which Cm-*BBX24* acts in the two intersecting pathways will provide a better understanding of the modulation of reproductive development in plants under abiotic stress conditions.

METHODS

Plant Materials and Treatments

A popular ground-cover chrysanthemum cultivar (*Chrysanthemum morifolium* cv Fall Color) with pink flowers was used as the wild-type control in this study. Chrysanthemum plants were propagated by in vitro culture for 50 d, then transplanted into 9-cm-diameter pots containing a mixture of 1:1 (v/v) of peat and vermiculite and transferred to a controlled temperature culture room with normal conditions (23 ± 1°C, 40% relative humidity, and 100 $\mu mol \cdot m^{-2} \cdot s^{-1}$ illumination by fluorescent lamps) under a LD cycle (16 h light/8 h dark). It should be noted that the fluorescent lamps produced a far-red light irradiance of only ~3% of the total irradiance. When the plants had seven to nine fully expanded leaves they were root-washed and placed in distilled water for 24 h for subsequent experiments.

Cm-*BBX24* Gene Isolation

Plants were transferred to a 4°C chamber for 6 h. Total RNA samples were extracted from whole plants using the Trizol reagent (Invitrogen) according to the manufacturer's instructions. Using the DREB1A regulon cDNA library obtained by suppression subtractive hybridization (Ma et al., 2010), 5′- and 3′-rapid amplification of cDNA ends was performed to isolate the 5′ and the 3′ cDNA ends of Cm-*BBX24* using the SMARTer RACE cDNA amplification kit (Clontech) according to the manufacturer's instructions. The full length of Cm-*BBX24* was obtained using gene-specific primers (Supplemental Table 3). The resulting PCR product was purified and cloned into the pGEM-T Easy Vector (Promega) for sequencing. Multiple sequence alignments were constructed using the ClustalW (http://www.ch.embnet.org/software/ClustalW.html) programs and BioEdit (http://www.mbio.ncsu.edu/BioEdit/bioedit.html).

Phylogenetic Analysis

The protein sequences of Cm-BBX24 and 8 structure group IV BBXs from *Arabidopsis thaliana* were multiply aligned using MUSCLE algorithm (gap open, 22.9; gap extend, 0; hydrophobicity multiplier, 1.5; clustering method, upgmb). The alignment used for the analysis is available as Supplemental Data Set 2. A phylogenetic analysis was conducted by MEGA version 4 (Tamura et al., 2007) using the neighbor-joining method with 1000 bootstrap replications.

Abiotic Stress Treatment of Chrysanthemum

For the freezing treatments, plants were transferred to a −6°C chamber for 8 h and then returned to 23°C for 30 d. For drought treatments, the plants were given adequate water and then water was withheld for 23 d and rewatered regularly and allowed to recover for 30 d. For the salt treatment, plants were transferred to a container filled with 400 mM NaCl solution for 4 weeks. The initial height of the solution was noted and maintained each day. Survival rates were recorded after the treatments finished and the plants were photographed to record their phenotypes.

Chrysanthemum Transformation

To construct the overexpression vector, the ORF sequence of Cm-*BBX24* was amplified using a pair of primers with *Xba*I and *Sma*I sites (Supplemental Table 3), and the resulting PCR product was digested with *Xba*I and *Sma*I and then cloned into the pBIG vector (Becker, 1990). To construct the RNAi vector, 361-bp sense and antisense fragments of Cm-*BBX24* containing *Xho*I/*Eco*RI and *Xba*I/*Hin*dIII sites were amplified and the two PCR products were digested with the corresponding restriction enzymes, as above, and directionally inserted into the two sides of the Pdk Intron in the pHANNIBAL vector step-by-step to form intron-containing hairpin RNA constructs. The intron-containing hairpin RNA construct with promoter and terminator was then subcloned into the binary vector pART27 (Wesley et al., 2001). The overexpression and RNAi plasmids were separately introduced into *Agrobacterium tumefaciens* strain LBA4404 and transformed into chrysanthemum by *Agrobacterium*-mediated transformation (Hong et al., 2006).

Phenotypic Characterization of Transgenic Chrysanthemum

The plants were considered to be entering the flowering stage when at least 50% of the ray flowers on at least one inflorescence were reflexed (Blanchard and Runkle, 2009). The times of first visible flower buds and first flower opening were recorded. For observation of flower bud differentiation, stem apices of Cm-*BBX24*-OX, wild-type, and Cm-*BBX24*-RNAi plants were isolated, paraffin embedded, and sectioned.

RNA-seq Analysis

Total RNA samples were extracted from the aerial parts of 4-week-old Cm-*BBX24*–overexpressing plants (line Cm-*BBX24*-OX-23), Cm-*BBX24* RNAi plants (line Cm-*BBX24*-RNAi-1), and wild-type plants, grown under normal conditions, using the RNeasy plant mini kit (Qiagen). Triplicate samples, comprising three independent plants of each line, were taken at ZT3. The RNA sequencing library was prepared as described by Zhong et al. (2011), and sequencing was performed on an Illumina HiSequation 2000 in the Genomics Facility of the Institute of Biotechnology, Cornell University (http://www.biotech.cornell.edu/).

RNA-seq Data Processing, de Novo Assembly, and Annotation

RNA-seq reads were first processed with a custom R script based on the ShortRead package to trim low quality (Q value < 20) nucleotides on both

ends and to clip the adapter and barcode sequences from the 3′ end. The resulting reads with lengths <40 bp or containing more than two ambiguous ("N") nucleotides were discarded. The RNA-seq reads were then aligned to GenBank virus (version 186) and the rRNA sequence databases using BWA and default parameters. Reads mapped to these two databases were discarded. The resulting high-quality cleaned reads were assembled de novo into contigs using Trinity with strand specific option "–SS_lib_type" set to "F" and "min_kmer_cov" set to 2 (Grabherr et al., 2011). To remove the redundancy of Trinity-generated contigs, they were further assembled de novo using iAssembler with minimum percent identify (-p) set to 99 (Zheng et al., 2011).

The resulting unique transcripts were screened by BLAST against the GenBank nonredundant (nr), UniProt (Swiss-Prot and TrEMBL), and *Arabidopsis* protein databases with a cutoff E-value of 1e-5. Gene Ontology terms were assigned to the chrysanthemum assembled transcripts based on the Gene Ontology terms annotated to their corresponding homologs in the UniProt database.

qRT-PCR Analysis

For the spatiotemporal expression analysis of Cm-*BBX24*, leaves, stems, roots, shoot apices at the vegetative growth stage and flower bud differentiation stage, flower buds, and flowers were taken from wild-type chrysanthemum grown under LD (16 h light/8 h dark). Three replicate samples were taken.

For the abiotic stress induction analysis of Cm-*BBX24*, the root-washed chrysanthemum plants were exposed for fixed times to the following conditions: control (distilled water treatment under LD and normal growth conditions); cold (chilling at 4°C in a growth chamber); dehydration (air drying on filter paper at room temperature); and salt (125 mM NaCl treatment under normal growth conditions). Shoots were then harvested and stored at −80°C prior to RNA extraction. The treatments were started at ZT3, and three replicate samples were taken.

To analyze the effect of daylength and $GA_{4/7}$ application on the expression patterns of Cm-*BBX24* and Cm-*FT*, we transferred wild-type chrysanthemum plants grown under LD for 2 weeks, to SD (8 h light/16 h dark) or kept under LD for 15 d, with or without a 100 μM GA_{4+7} treatment once every 3 d. Samples were collected at ZT3 with 3-d intervals and three replicate samples were taken. To detect correlations in the expression of Cm-*BBX24* and floral integrators under different daylengths, Cm-*BBX24*-RNAi and wild-type chrysanthemum plants grown under LD for 2 weeks were transferred to SD or kept under LD for 9 d. Samples were collected at ZT3 with 3-d intervals, and three replicate samples were taken.

Total RNA samples were extracted from the above sample stock using the Trizol agent, as above, and cDNAs were synthesized from 1 μg total RNA using M-MLV reverse transcriptase (Promega). qRT-PCR reactions (20 μL volume containing 2 μL cDNA as the template) were performed using the StepOne real-time PCR system (Applied Biosystems) in standard mode with the KAPA SYBR FAST Universal qRT-PCR kit (Kapa Biosystems). All reactions were performed in triplicate, and the chrysanthemum *Ubiquitin* gene was used as the internal control. PCR primers are listed in Supplemental Table 3.

Subcellular Localization Analysis of Cm-BBX24

A cDNA fragment containing the ORF of Cm-*BBX24* (stop codon removed) was amplified using a pair of primers containing *Eco*RI or *Sal*I sites (Supplemental Table 3). The PCR products were digested with *Eco*RI and *Sal*I and then cloned into the pEZS-NL vector (D. Ehrhardt, http://deepgreen.stanford.edu), which resulted in the Cm-*BBX24* coding sequence fused in frame with the 5′ terminus of a sequence encoding GFP, driven by the cauliflower mosaic virus 35S promoter. The vector pEZS-NL deleted Ala (10) linker containing 35S:GFP was used as a control. Plasmids were individually transformed into onion epidermal cells using a particle bombardment method. Transformed onion epidermal cells were cultured on Murashige and Skoog media in dark conditions for 24 to 30 h at 22°C and were observed using a confocal laser scanning microscope (Nikon C1 Plus).

Transactivation Analysis of Cm-BBX24 in Yeast Cells

The ORF (1 to 245 amino acids), B-box domain at the N terminus (1 to 95 amino acids), and the C terminus (96 to 245 amino acids) of the Cm-*BBX24* gene were amplified using three pairs of primers with *Eco*RI and *Sal*I sites. The primers are listed in Supplemental Table 3. The PCR products were digested with *Eco*RI and *Sal*I and were then cloned into the DNA binding domain vector pBD-GAL4 Cam (Clontech) to yield the expression vectors pBD-Cm-*BBX24*, pBD-Cm-*BBX24*N, and pBD-Cm-*BBX24*C. pBD-GAL4 and pGAL4 were used as negative and positive controls, respectively. The constructs were transformed into yeast (*Saccharomyces cerevisiae*) strain YRG-2 containing the reporter genes *LacZ* and *HIS3*, according to the method described in the Yeast Protocols Handbook PT3024-1 (Clontech). The yeast transformants were incubated at 30°C for 3 d on SD deleting tryptophan medium with or without histidine. The transformed yeast cells were then transferred to filter paper and incubated at 30°C for 3 to 8 h in the presence of X-gal to assess the presence of β-galactosidase by observing blue color formation. A quantitative β-galactosidase assay was also performed also using *o*-nitrophenyl β-D-galactopyranoside, according to the method described in the Yeast Protocols Handbook PT3024-1. Three transformants were selected and subjected to the β-galactosidase assay.

The Determination of GA Content in Transgenic Chrysanthemum Leaves

Cm-*BBX24*-OX/RNAi and wild-type plants were grown under LD for 40 d and then were transferred to SD or kept in LD for 3 d. Three replicate leaf samples were taken from each line, and each leaf sample was from top three fully opened leaves, and harvest time was 3 h after the lights were turned on. Leaf tissue GA concentrations (expressed as ng/g fresh weight [FW] of leaf tissue extracted) were analyzed by the stable isotope dilution method as described by M.L. Chen et al. (2012).

Each sample (100 mg FW) was extracted with 1.0 mL 80% methanol (v/v) at 4°C for 12 h. As internal standards, $[^2H_2]$ GA_1 (1.0 ng/g), $[^2H_2]$ GA_3 (1.0 ng/g), $[^2H_2]$ GA_4 (1.0 ng/g), $[^2H_2]$ GA_5 (1.0 ng/g), $[^2H_2]$ GA_8 (1.0 ng/g), $[^2H_2]$ GA_{19} (1.0 ng/g), $[^2H_2]$ GA_{20} (1.0 ng/g), $[^2H_2]$ GA_{24} (1.0 ng/g), $[^2H_2]$ GA_{34} (1.0 ng/g), $[^2H_2]$ GA_{51} (1.0 ng/g), and $[^2H_2]$ GA_{53} (1.0 ng/g) were added to the samples before grinding. After centrifugation (10,000*g*, 4°C, 20 min), the supernatants were collected and then passed through the tandem SPE cartridges containing C_{18} sorbent (50 mg) and SAX sorbent (200 mg). After sample loading, the C_{18} cartridge was removed and the SAX cartridge was rinsed with 2 mL methanol/water (20/80, v/v). Three milliliters of acetonitrile (ACN) with 1% formic acid (v/v) was applied to dilute the targeted acidic phytohormones, and the diluents were evaporated and then redissolved in 100 μL water. The resulting solution was then acidified with 10 μL formic acid and extracted with ether (2 × 1 mL). The ether phase was combined, dried under nitrogen gas, and reconstituted in 100 μL ACN. Subsequently, 10 μL triethylamine (20 μmol/mL) and 10 μL 3-bromoactonyltrimethylammonium bromide (20 μmol/mL) were added. The reaction solution was vortexed for 30 min at 35°C and evaporated under nitrogen gas and then redissolved in 200 μL water/ACN (90/10, v/v) for further analysis (M.L. Chen et al., 2012).

GA Treatment of Chrysanthemum

For flower bud observation, wild-type and Cm-*BBX24*-OX/RNAi plants were grown under LD for 30 d and then transferred to SD or kept under LD before spraying with 100 μM $GA_{4/7}$. The $GA_{4/7}$ was dissolved in absolute

ethanol, and a 1000-fold dilution was used for the spray application experiment. The same concentration of ethanol solution was used as a mock control. The $GA_{4/7}$ treatment was performed twice per week until the flower buds emerged.

Electrolyte Leakage

Chrysanthemum plants were grown at 23°C under LD and then sprayed three times with 100 μM GA_{4+7}, once every 3 d. Plants with/without GA treatment were then transferred to −2°C chamber for 48 h. Leaves were harvested from the middle of the stem, and electrolyte leakage was determined according to the method of Leopold et al. (1981).

Accession Numbers

Sequence data from this article can be found in the Arabidopsis Genome Initiative or GenBank/EMBL databases under the following accession numbers: Cm-*BBX24*, *C. morifolium*, KF385866; the raw sequence reads of RNA-seq, *C. morifolium*, SRP038981 and SRA091277; At-BBX24, *Arabidopsis*, NP172094, At1g06040; At-BBX25, *Arabidopsis*, NP565722, At2g31380; Gm-BBX24, *Glycine max*, ABB29467; Br-BBX24, *Brassica rapa*, ABV89657; Ss-BBX24, *Solanum sogarandinum*, ABC25454; Cm-BBX24, *Cucumis melo*, ADN34088; Rc-BBX24, *Ricinus communis*, XP002534139; Os-BBX24, *Oryza sativa*, CAH67738; At-BBX18, *Arabidopsis*, NP565507, At2g21320; At-BBX19, *Arabidopsis*, NP195607, At4g38960; At-BBX20, *Arabidopsis*, NP195618, At4g39070; At-BBX21, *Arabidopsis*, NP177686, At1g75540; AtBBX22, *Arabidopsis*, NP565183, At1g78600; AtBBX23, *Arabidopsis*, NP192762, At4g10240; Cm-*Ubiquitin*, *C. morifolium*, EU862325; Cs-*AFT*, *C. seticuspe*, AB839766; Cs-*TFL1*, *C. seticuspe*, AB839767; Cs-*FTL1*, *C. seticuspe*, AB545936; Cs-*FTL2*, *C. seticuspe*, AB679271; Cs-*FTL3*, *C. seticuspe*, AB679272; *GI*, *Arabidopsis*, NM102124, At1g22770; *CO*, *Arabidopsis*, NM001036810, At5g15840; *FT*, *Arabidopsis*, NM1052, At1G65480; *SOC1*, *Arabidopsis*, NM130128, At2g45660; *GA20ox1*, *Arabidopsis*, NM118674, At4g25420; *GA20ox2*, *Arabidopsis*, NM124560, At5g51810; *GA20ox3*, *Arabidopsis*, NM120802, At5g07200; *GA20ox4*, *Arabidopsis*, NM104778, At1g60980; *GA20ox5*, *Arabidopsis*, NM103535, At1g44090; *GA3ox1*, *Arabidopsis*, NM101424, At1g15550; *GA3ox2*, *Arabidopsis*, NM106683, At1g80340; *GA2ox1*, *Arabidopsis*, NM106491, At1g78440; *GA2ox2*, *Arabidopsis*, NM001036035, At1g30040; *GA2ox3*, *Arabidopsis*, NM129007, At2g34555; *GA2ox4*, *Arabidopsis*, NM103695, At1g47990; *GA2ox6*, *Arabidopsis*, NM100121, AT1g02400; *GA2ox7*, *Arabidopsis*, NM103976, At1g50960; *GA2ox8*, *Arabidopsis*, NM101973, At1g21200.

Supplemental Data

The following materials are available in the online version of this article.

Supplemental Figure 1. Activities of the Cm-*BBX24* Promoter in Response to Hormone Treatments and Abiotic Stresses in Transgenic *Arabidopsis* Plants.

Supplemental Figure 2. Relative Expression of Cm-*BBX24* Transcripts under the Control of the Circadian Clock and Different Daylengths.

Supplemental Figure 3. Comparison of the Expression of Cm-*BBX24* and Other Members of BBX Structure Group IV in Cm-*BBX24*-RNAi and Wild-Type Chrysanthemum Plants.

Supplemental Figure 4. Flowering Time of Cm-*BBX24*–Overexpressing *Arabidopsis* Plants.

Supplemental Figure 5. The Number of Assembled Transcripts Differentially Expressed between Cm-*BBX24*-OX, Cm-*BBX24*-RNAi, and Wild-Type Chrysanthemum Plants.

Supplemental Figure 6. Expression of the Photoperiod Pathway and GA Biosynthesis Pathway-Relevant Genes and Effect of $GA_{4/7}$ Treatment on Flowering Time in Transgenic *Arabidopsis* and Chrysanthemum Plants.

Supplemental Figure 7. Schematic Model Describing the Involvement of Cm-*BBX24* in Flowering and Abiotic Stress Tolerance in Chrysanthemum.

Supplemental Table 1. Annotation of Genes Upregulated in Cm-*BBX24*-OX Plants but Downregulated in Cm-*BBX24*-RNAi Plants.

Supplemental Table 2. Differentially Expressed Genes in Cm-*BBX24*-OX/RNAi and Wild-Type Chrysanthemum Plants by qRT-PCR Analysis.

Supplemental Table 3. Primers Used for Gene Isolation, qRT-PCR Analysis, and Vector Construction.

Supplemental Data Set 1. List of Assembled Transcripts Upregulated or Downregulated (>2.0-Fold, Adjusted $P < 0.05$) in Cm-*BBX24* Transgenic Chrysanthemum Plants, Relative to Wild-Type Plants.

Supplemental Data Set 2. Text File of the Alignment Used for the Phylogenetic Analysis of Group IV BBXs Shown in Figure 1B.

ACKNOWLEDGMENTS

We acknowledge PlantScribe (www.plantscribe.com) for careful editing of this article. This work was supported by the National Natural Science Foundation of China (Grants 31372094, 31171990, and 91217309).

AUTHOR CONTRIBUTIONS

Y.Y. performed the experiments and wrote the article. C.M., Y.X., Q.W., M.I., H.L., L.C., and M.W. helped with experiments. S.G. and Z.F. analyzed the data. B.H. and J.G. conceived and designed the experiments and wrote the article. All authors read and approved the final article.

Received March 1, 2014; revised April 8, 2014; accepted April 16, 2014; published May 23, 2014.

REFERENCES

Achard, P., Gong, F., Cheminant, S., Alioua, M., Hedden, P., and Genschik, P. (2008). The cold-inducible CBF1 factor-dependent signaling pathway modulates the accumulation of the growth-repressing DELLA proteins via its effect on gibberellin metabolism. Plant Cell **20:** 2117–2129.

Avonce, N., Leyman, B., Mascorro-Gallardo, J.O., Van Dijck, P., Thevelein, J.M., and Iturriaga, G. (2004). The Arabidopsis trehalose-6-P synthase *AtTPS1* gene is a regulator of glucose, abscisic acid, and stress signaling. Plant Physiol. **136:** 3649–3659.

Becker, D. (1990). Binary vectors which allow the exchange of plant selectable markers and reporter genes. Nucleic Acids Res. **18:** 203.

Blanchard, M.G., and Runkle, E.S. (2009). Use of a cyclic high-pressure sodium lamp to inhibit flowering of chrysanthemum and velvet sage. Sci. Hortic. (Amsterdam) **122:** 448–454.

Blázquez, M.A., Green, R., Nilsson, O., Sussman, M.R., and Weigel, D. (1998). Gibberellins promote flowering of Arabidopsis by activating the *LEAFY* promoter. Plant Cell **10:** 791–800.

Cao, S., Ye, M., and Jiang, S. (2005). Involvement of *GIGANTEA* gene in the regulation of the cold stress response in Arabidopsis. Plant Cell Rep. **24:** 683–690.

Chen, J., Chen, J.Y., Wang, J.N., Kuang, J.F., Shan, W., and Lu, W.J. (2012). Molecular characterization and expression profiles of *MaCOL1*, a *CONSTANS*-like gene in banana fruit. Gene **496:** 110–117.

Chen, M.L., Fu, X.M., Liu, J.Q., Ye, T.T., Hou, S.Y., Huang, Y.Q., Yuan, B.F., Wu, Y., and Feng, Y.Q. (2012). Highly sensitive and quantitative profiling of acidic phytohormones using derivatization approach coupled with nano-LC-ESI-Q-TOF-MS analysis. J. Chromatogr. B Analyt. Technol. Biomed. Life Sci. **905:** 67–74.

Cheng, X.F., and Wang, Z.Y. (2005). Overexpression of *COL9*, a *CONSTANS-LIKE* gene, delays flowering by reducing expression of *CO* and *FT* in *Arabidopsis thaliana.* Plant J. **43:** 758–768.

Cockshull, K.E. (1985). *Chrysanthemum morifolium*. In CRC Handbook of Flowering, Vol. II, A.H. Halevy, ed (Boca Raton, FL: CRC), pp. 238–257.

Coles, J.P., Phillips, A.L., Croker, S.J., García-Lepe, R., Lewis, M.J., and Hedden, P. (1999). Modification of gibberellin production and plant development in Arabidopsis by sense and antisense expression of gibberellin 20-oxidase genes. Plant J. **17:** 547–556.

Cortina, C., and Culianez-Macia, F.A. (2005). Tomato abiotic stress enhanced tolerance by trehalose biosynthesis. Plant Sci. **169:** 75–82.

Dill, A., and Sun, T.P. (2001). Synergistic derepression of gibberellin signaling by removing RGA and GAI function in *Arabidopsis thaliana*. Genetics **159:** 777–785.

Eriksson, S., Böhlenius, H., Moritz, T., and Nilsson, O. (2006). GA_4 is the active gibberellin in the regulation of LEAFY transcription and Arabidopsis floral initiation. Plant Cell **18:** 2172–2181.

Evans, L.T., and King, R.W. (1985). *Lolium temulentum*. In CRC Handbook of Flowering, A.H. Halevy, ed (Boca Raton, FL: CRC Press), pp. 306–323.

Fornara, F., de Montaigu, A., and Coupland, G. (2010). SnapShot: Control of flowering in Arabidopsis. Cell **141:** 550, e1–e2.

Fowler, S., Lee, K., Onouchi, H., Samach, A., Richardson, K., Morris, B., Coupland, G., and Putterill, J. (1999). *GIGANTEA*: a circadian clock-controlled gene that regulates photoperiodic flowering in Arabidopsis and encodes a protein with several possible membrane-spanning domains. EMBO J. **18:** 4679–4688.

Grabherr, M.G., et al. (2011). Full-length transcriptome assembly from RNA-Seq data without a reference genome. Nat. Biotechnol. **29:** 644–652.

Han, Y., Zhang, X., Wang, Y., and Ming, F. (2013). The suppression of WRKY44 by GIGANTEA-miR172 pathway is involved in drought response of *Arabidopsis thaliana.* PLoS ONE **8:** e73541.

Hassidim, M., Harir, Y., Yakir, E., Kron, I., and Green, R.M. (2009). Over-expression of *CONSTANS-LIKE 5* can induce flowering in short-day grown Arabidopsis. Planta **230:** 481–491.

Hedden, P., and Phillips, A.L. (2000). Gibberellin metabolism: new insights revealed by the genes. Trends Plant Sci. **5:** 523–530.

Higuchi, Y., Narumi, T., Oda, A., Nakano, Y., Sumitomo, K., Fukai, S., and Hisamatsu, T. (2013). The gated induction system of a systemic floral inhibitor, antiflorigen, determines obligate short-day flowering in chrysanthemums. Proc. Natl. Acad. Sci. USA **110:** 17137–17142.

Hirayama, T., and Shinozaki, K. (2010). Research on plant abiotic stress responses in the post-genome era: past, present and future. Plant J. **61:** 1041–1052.

Hong, B., Tong, Z., Ma, N., Kasuga, M., Yamaguchi-Shinozaki, K., and Gao, J.P. (2006). Expression of Arabidopsis *DREB1A* gene in transgenic chrysanthemum enhances tolerance to low temperature. J. Hortic. Sci. Biotechnol. **81:** 1002–1008.

Hong, S.W., Jon, J.H., Kwak, J.M., and Nam, H.G. (1997). Identification of a receptor-like protein kinase gene rapidly induced by abscisic acid, dehydration, high salt, and cold treatments in *Arabidopsis thaliana*. Plant Physiol. **113:** 1203–1212.

Huerta, L., Forment, J., Gadea, J., Fagoaga, C., Peña, L., Pérez-Amador, M.A., and García-Martínez, J.L. (2008). Gene expression analysis in citrus reveals the role of gibberellins on photosynthesis and stress. Plant Cell Environ. **31:** 1620–1633.

Jiang, S.Y., Ma, Z., and Ramachandran, S. (2010). Evolutionary history and stress regulation of the lectin superfamily in higher plants. BMC Evol. Biol. **10:** 79–103.

Kader, M.A., and Lindberg, S. (2010). Cytosolic calcium and pH signaling in plants under salinity stress. Plant Signal. Behav. **5:** 233–238.

Kania, T., Russenberger, D., Peng, S., Apel, K., and Melzer, S. (1997). FPF1 promotes flowering in Arabidopsis. Plant Cell **9:** 1327–1338.

Khanna, R., Kronmiller, B., Maszle, D.R., Coupland, G., Holm, M., Mizuno, T., and Wu, S.H. (2009). The Arabidopsis B-box zinc finger family. Plant Cell **21:** 3416–3420.

Kim, S.K., Yun, C.H., Lee, J.H., Jang, Y.H., Park, H.Y., and Kim, J.K. (2008). *OsCO3*, a *CONSTANS*-LIKE gene, controls flowering by negatively regulating the expression of *FT*-like genes under SD conditions in rice. Planta **228:** 355–365.

King, R.W. (2012). Mobile signals in day length_regulated flowering: gibberellins, flowering Locus T, and sucrose. Russ. J. Plant Physiol. **59:** 479–490.

King, R.W., Evans, L.T., Mander, L.N., Moritz, T., Pharis, R.P., and Twitchin, B. (2003). Synthesis of gibberellin GA_6 and its role in flowering of *Lolium temulentum.* Phytochemistry **62:** 77–82.

King, R.W., Moritz, T., Evans, L.T., Junttila, O., and Herlt, A.J. (2001). Long-day induction of flowering in *Lolium temulentum* involves sequential increases in specific gibberellins at the shoot apex. Plant Physiol. **127:** 624–632.

King, R.W., Moritz, T., Evans, L.T., Martin, J., Andersen, C.H., Blundell, C., Kardailsky, I., and Chandler, P.M. (2006). Regulation of flowering in the long-day grass Lolium temulentum by gibberellins and the *FLOWERING LOCUS T* gene. Plant Physiol. **141:** 498–507.

Kurepin, L.V., Dahal, K.P., Savitch, L.V., Singh, J., Bode, R., Ivanov, A.G., Hurry, V., and Hüner, N.P. (2013). Role of CBFs as integrators of chloroplast redox, phytochrome and plant hormone signaling during cold acclimation. Int. J. Mol. Sci. **14:** 12729–12763.

Lang, A. (1965). Physiology of flower initation. In Encyclopedia of Plant Physiology, W. Ruhland, ed (Berlin, Heidelberg, New York: Springer-Verlag), pp. 1380–1536.

Langridge, J. (1957). Effect of day-length and gibberellic acid on the flowering of Arabidopsis. Nature **180:** 36–37.

Leopold, A.C., Musgrave, M.E., and Williams, K.M. (1981). Solute leakage resulting from leaf desiccation. Plant Physiol. **68:** 1222–1225.

Lippuner, V., Cyert, M.S., and Gasser, C.S. (1996). Two classes of plant cDNA clones differentially complement yeast calcineurin mutants and increase salt tolerance of wild-type yeast. J. Biol. Chem. **271:** 12859–12866.

Ma, C., Hong, B., Wang, T., Yang, Y.J., Tong, Z., Zuo, Z.R., Yamaguchi-Shinozaki, K., and Gao, J.P. (2010). DREB1A regulon expression in *rd29A:DREB1A* transgenic chrysanthemum under low temperature or dehydration stress. J. Hortic. Sci. Biotechnol. **85:** 503–510.

Moon, J., Suh, S.S., Lee, H., Choi, K.R., Hong, C.B., Paek, N.C., Kim, S.G., and Lee, I. (2003). The *SOC1* MADS-box gene integrates vernalization and gibberellin signals for flowering in Arabidopsis. Plant J. **35:** 613–623.

Mouradov, A., Cremer, F., and Coupland, G. (2002). Control of flowering time: interacting pathways as a basis for diversity. Plant Cell **14** (suppl.): 111–130.

Nagaoka, S., and Takano, T. (2003). Salt tolerance-related protein STO binds to a Myb transcription factor homologue and confers salt tolerance in Arabidopsis. J. Exp. Bot. **54:** 2231–2237.

Nakamichi, N., Kusano, M., Fukushima, A., Kita, M., Ito, S., Yamashino, T., Saito, K., Sakakibara, H., and Mizuno, T. (2009). Transcript profiling of an Arabidopsis PSEUDO RESPONSE REGULATOR arrhythmic triple

mutant reveals a role for the circadian clock in cold stress response. Plant Cell Physiol. **50:** 447–462.

Nakano, Y., Higuchi, Y., Sumitomo, K., and Hisamatsu, T. (2013). Flowering retardation by high temperature in chrysanthemums: involvement of *FLOWERING LOCUS T-like 3* gene repression. J. Exp. Bot. **64:** 909–920.

Olszewski, N., Sun, T.P., and Gubler, F. (2002). Gibberellin signaling: biosynthesis, catabolism, and response pathways. Plant Cell **14** (suppl.)**:** S61–S80.

Oda, A., Narumi, T., Li, T., Kando, T., Higuchi, Y., Sumitomo, K., Fukai, S., and Hisamatsu, T. (2012). *CsFTL3*, a chrysanthemum *FLOWERING LOCUS T*-like gene, is a key regulator of photoperiodic flowering in chrysanthemums. J. Exp. Bot. **63:** 1461–1477.

Park, H.Y., Lee, S.Y., Seok, H.Y., Kim, S.H., Sung, Z.R., and Moon, Y.H. (2011). EMF1 interacts with EIP1, EIP6 or EIP9 involved in the regulation of flowering time in Arabidopsis. Plant Cell Physiol. **52:** 1376–1388.

Pharis, R.P. (1972). Flowering of Chrysanthemum under non-inductive long days by gibberellins and N(^{6})-benzyladenine. Planta **105:** 205–212.

Pharis, R.P., and King, R.W. (1985). Gibberellins and reproductive deve in seed plants. Annu. Rev. Plant Physiol. **36:** 517–568.

Pimenta Lange, M.J., and Lange, T. (2006). Gibberellin biosynthesis and the regulation of plant development. Plant Biol (Stuttg) **8:** 281–290.

Porri, A., Torti, S., Romera-Branchat, M., and Coupland, G. (2012). Spatially distinct regulatory roles for gibberellins in the promotion of flowering of Arabidopsis under long photoperiods. Development **139:** 2198–2209.

Putterill, J., Robson, F., Lee, K., Simon, R., and Coupland, G. (1995). The *CONSTANS* gene of Arabidopsis promotes flowering and encodes a protein showing similarities to zinc finger transcription factors. Cell **80:** 847–857.

Robson, F., Costa, M.M., Hepworth, S.R., Vizir, I., Piñeiro, M., Reeves, P.H., Putterill, J., and Coupland, G. (2001). Functional importance of conserved domains in the flowering-time gene *CONSTANS* demonstrated by analysis of mutant alleles and transgenic plants. Plant J. **28:** 619–631.

Samach, A., Onouchi, H., Gold, S.E., Ditta, G.S., Schwarz-Sommer, Z., Yanofsky, M.F., and Coupland, G. (2000). Distinct roles of CONSTANS target genes in reproductive development of Arabidopsis. Science **288:** 1613–1616.

Seki, M., et al. (2002). Monitoring the expression profiles of 7000 Arabidopsis genes under drought, cold and high-salinity stresses using a full-length cDNA microarray. Plant J. **31:** 279–292.

Seo, E., Lee, H., Jeon, J., Park, H., Kim, J., Noh, Y.S., and Lee, I. (2009). Crosstalk between cold response and flowering in Arabidopsis is mediated through the flowering-time gene *SOC1* and its upstream negative regulator *FLC.* Plant Cell **21:** 3185–3197.

Song, Y.H., Ito, S., and Imaizumi, T. (2013). Flowering time regulation: photoperiod- and temperature-sensing in leaves. Trends Plant Sci. **18:** 575–583.

Srikanth, A., and Schmid, M. (2011). Regulation of flowering time: all roads lead to Rome. Cell. Mol. Life Sci. **68:** 2013–2037.

Sumitomo, K., Li, T., and Hisamatsu, T. (2009). Gibberellin promotes flowering of chrysanthemum by upregulating *CmFL*, a chrysanthemum *FLORICAULA/LEAFY* homologous gene. Plant Sci. **176:** 643–649.

Takuhara, Y., Kobayashi, M., and Suzuki, S. (2011). Low-temperature-induced transcription factors in grapevine enhance cold tolerance in transgenic Arabidopsis plants. J. Plant Physiol. **168:** 967–975.

Tamura, K., Dudley, J., Nei, M., and Kumar, S. (2007). MEGA4: molecular evolutionary genetics analysis (MEGA) software version 4.0. Mol. Biol. Evol. **24:** 1596–1599.

Todaka, D., Matsushima, H., and Morohashi, Y. (2000). Water stress enhances β-amylase activity in cucumber cotyledons. J. Exp. Bot. **51:** 739–745.

Wesley, S.V., et al. (2001). Construct design for efficient, effective and high-throughput gene silencing in plants. Plant J. **27:** 581–590.

Winter, D., Vinegar, B., Nahal, H., Ammar, R., Wilson, G.V., and Provart, N.J. (2007). An "Electronic Fluorescent Pictograph" browser for exploring and analyzing large-scale biological data sets. PLoS ONE **2:** e718.

Yamada, M., and Takeno, K. (2014). Stress and salicylic acid induce the expression of PnFT2 in the regulation of the stress-induced flowering of *Pharbitis nil.* J. Plant Physiol. **171:** 205–212.

Yamaguchi, S. (2008). Gibberellin metabolism and its regulation. Annu. Rev. Plant Biol. **59:** 225–251.

Yano, M., Katayose, Y., Ashikari, M., Yamanouchi, U., Monna, L., Fuse, T., Baba, T., Yamamoto, K., Umehara, Y., Nagamura, Y., and Sasaki, T. (2000). *Hd1*, a major photoperiod sensitivity quantitative trait locus in rice, is closely related to the Arabidopsis flowering time gene *CONSTANS.* Plant Cell **12:** 2473–2484.

Zhang, S., Yang, C., Peng, J., Sun, S., and Wang, X. (2009). GASA5, a regulator of flowering time and stem growth in *Arabidopsis thaliana.* Plant Mol. Biol. **69:** 745–759.

Zheng, Y., Zhao, L.J., Gao, J.P., and Fei, Z.J. (2011). iAssembler: a package for de novo assembly of Roche-454/Sanger transcriptome sequences. BMC Bioinformatics **12:** 453.

Zhong, S.L., Joung, J.G., Zheng, Y., Chen, Y.R., Liu, B., Shao, Y., Xiang, J.Z., Fei, Z.J., and Giovannoni, J.J. (2011). High-throughput illumina strand-specific RNA sequencing library preparation. Cold Spring Harb Protoc **2011:** 940–949.